

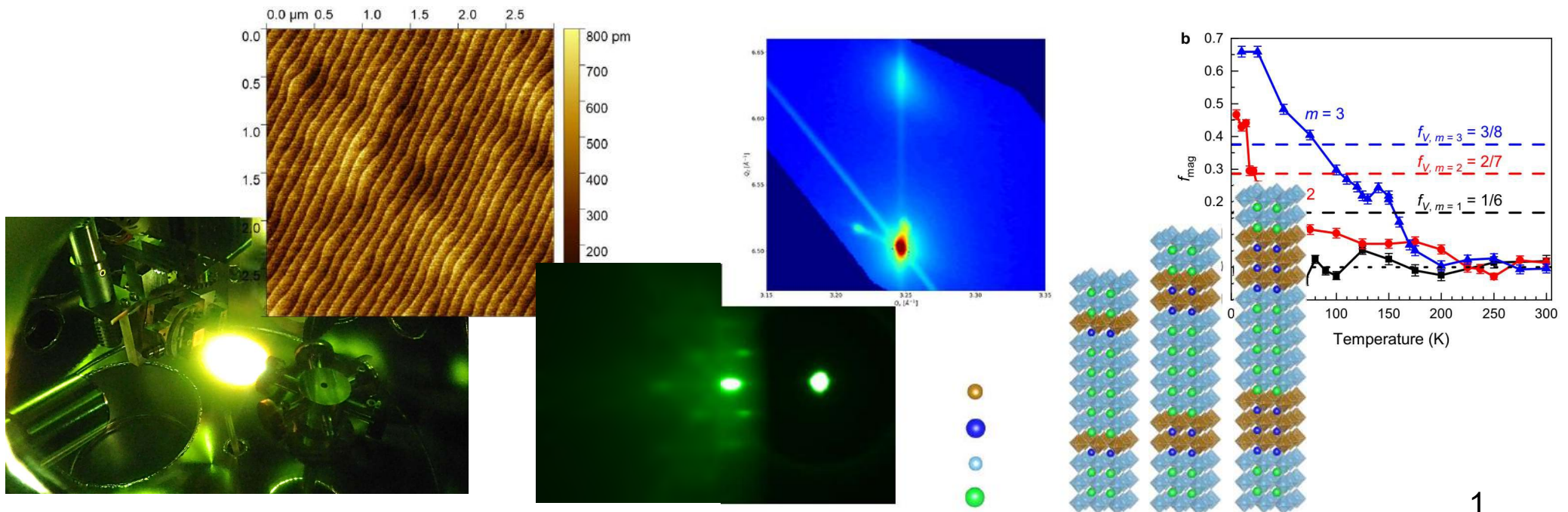
Pulsed laser deposition – principles and applications

MUNI
SCI



A. Dubroka, M. Kiaba, J. Klimek

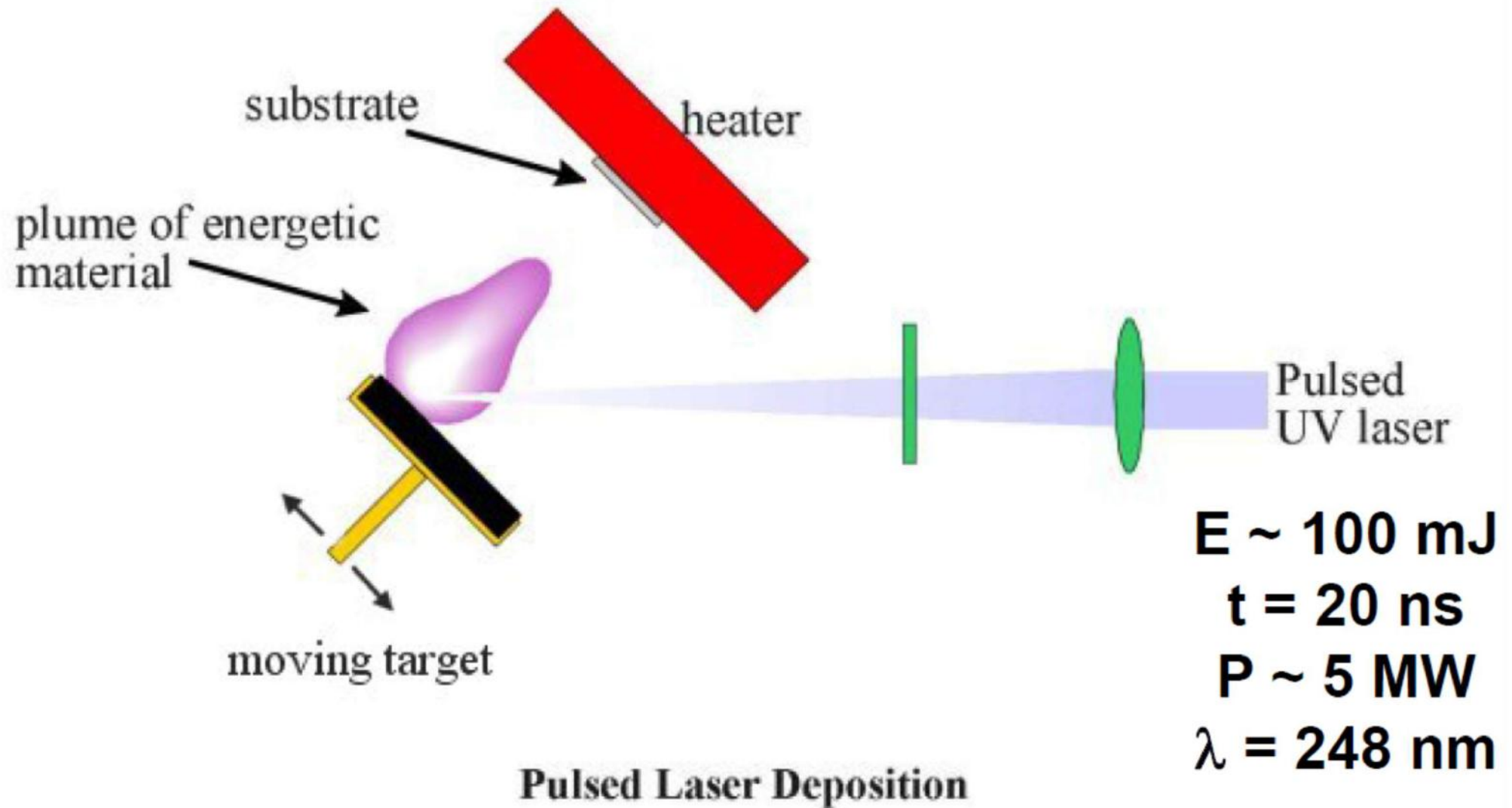
Institute of Condensed Matter Physics, Faculty of Science
Masaryk University, Kotlářská 2, Brno, Czech Republic



Overview of the talk

- Principle of pulsed laser deposition
- Transition metal oxides
- Examples of growth of thin films: $\text{La}_{0.7}\text{Sr}_{0.3}\text{MnO}_3$, LaCoO_3 , and $\text{La}_{0.3}\text{Sr}_{0.7}\text{CoO}_3$
- Reflection of high energy electron diffraction – principle and examples
- Example of deposition of $\text{LaFeO}_3/\text{SrTiO}_3$ superlattices

Principle of pulsed laser deposition



Pulse-laser deposition – advantages/disadvantages

Advantages:

- Deposition of epitaxial thin films
- Easy to grow complex compounds (oxides) in desired stoichiometric ratio
- Process is (relatively) simple and flexible
- Switching to a different compound is easy - exchange of a target
- Can hold multiple targets and easy to prepare multilayers and heterostructures
- Deposition of thin film can be done in short time

Disadvantages:

- No control of individual ion composition (compared to MBE)
- Not suitable for depositions of very large surfaces needed for industrial applications
- Not suitable for deposition of thick films
- For some materials, molten particles or target fragments are deposited in film

Transition metal oxides

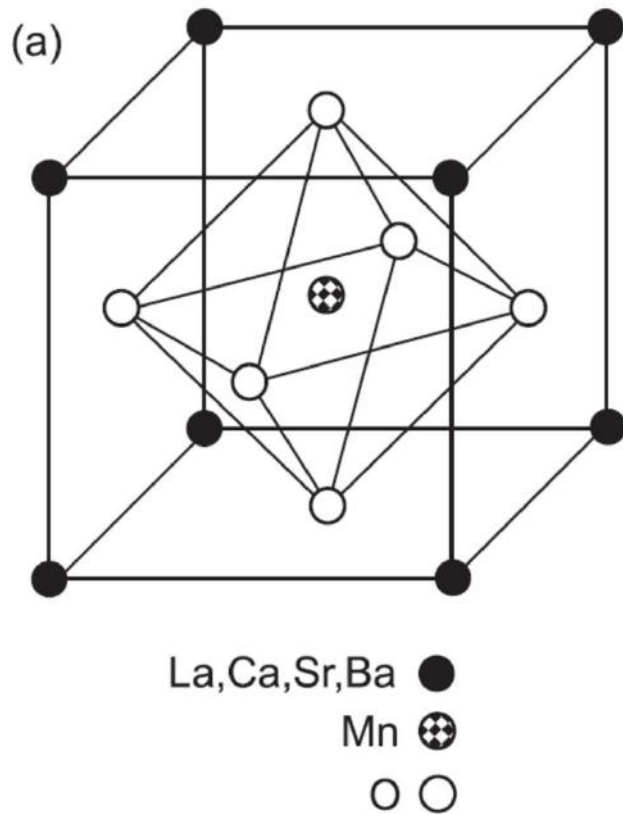
| Group→ ↓Period | 1 | 2 | 3 | 4 | 5 | 6 | 7 | 8 | 9 | 10 | 11 | 12 | 13 | 14 | 15 | 16 | 17 | 18 |
|-------------------|----------|----------|-----------------------------|-----------|-----------|-----------|-----------|-----------|-----------|-----------|-----------|-----------|------------|------------|------------|------------|------------|------------|
| 1 | 1 H | | | | | | | | | | | | | | | | | 2 He |
| 2 | 3 Li | 4 Be | Transition Metals (d-block) | | | | | | | | | | 5 B | 6 C | 7 N | 8 O | 9 F | 10 Ne |
| 3 | 11 Na | 12 Mg | | | | | | | | | | | 13 Al | 14 Si | 15 P | 16 S | 17 Cl | 18 Ar |
| 4 | 19 K | 20 Ca | 21 Sc | 22 Ti | 23 V | 24 Cr | 25 Mn | 26 Fe | 27 Co | 28 Ni | 29 Cu | 30 Zn | 31 Ga | 32 Ge | 33 As | 34 Se | 35 Br | 36 Kr |
| 5 | 37 Rb | 38 Sr | 39 Y | 40 Zr | 41 Nb | 42 Mo | 43 Tc | 44 Ru | 45 Rh | 46 Pd | 47 Ag | 48 Cd | 49 In | 50 Sn | 51 Sb | 52 Te | 53 I | 54 Xe |
| 6 | 55 Cs | 56 Ba | | 72 Hf | 73 Ta | 74 W | 75 Re | 76 Os | 77 Ir | 78 Pt | 79 Au | 80 Hg | 81 Tl | 82 Pb | 83 Bi | 84 Po | 85 At | 86 Rn |
| 7 | 87 Fr | 88 Ra | | 104 Rf | 105 Db | 106 Sg | 107 Bh | 108 Hs | 109 Mt | 110 Ds | 111 Rg | 112 Cn | 113 Uut | 114 Uuq | 115 Uup | 116 Uuh | 117 Uus | 118 Uuo |
| Lanthanides | | | 57 La | 58 Ce | 59 Pr | 60 Nd | 61 Pm | 62 Sm | 63 Eu | 64 Gd | 65 Tb | 66 Dy | 67 Ho | 68 Er | 69 Tm | 70 Yb | 71 Lu | |
| Actinides | | | 89 Ac | 90 Th | 91 Pa | 92 U | 93 Np | 94 Pu | 95 Am | 96 Cm | 97 Bk | 98 Cf | 99 Es | 100 Fm | 101 Md | 102 No | 103 Lr | |

Wide variety of (often exotic) material properties :

- superconductivity (oxides of Cu – $\text{YBa}_2\text{Cu}_3\text{O}_7\dots$)
- ferro- a antiferro -magnetism
(oxides of Mn, Co, Cr, Ni..., $\text{La}_{1-x}\text{Sr}_x\text{MnO}_3$)
- ferroelectricity (oxides of Ti, e.g. BaTiO_3)
- multiferroics ($\text{BiFeO}_3\dots$)
- insulator-metal transitions (oxides of Mn, $\text{La}_{1-x}\text{Sr}_x\text{MnO}_3$)
- semiconductors (SrTiO_3 , $\text{ZnO} \dots$)
- insulators ($\text{LaAlO}_3\dots$)

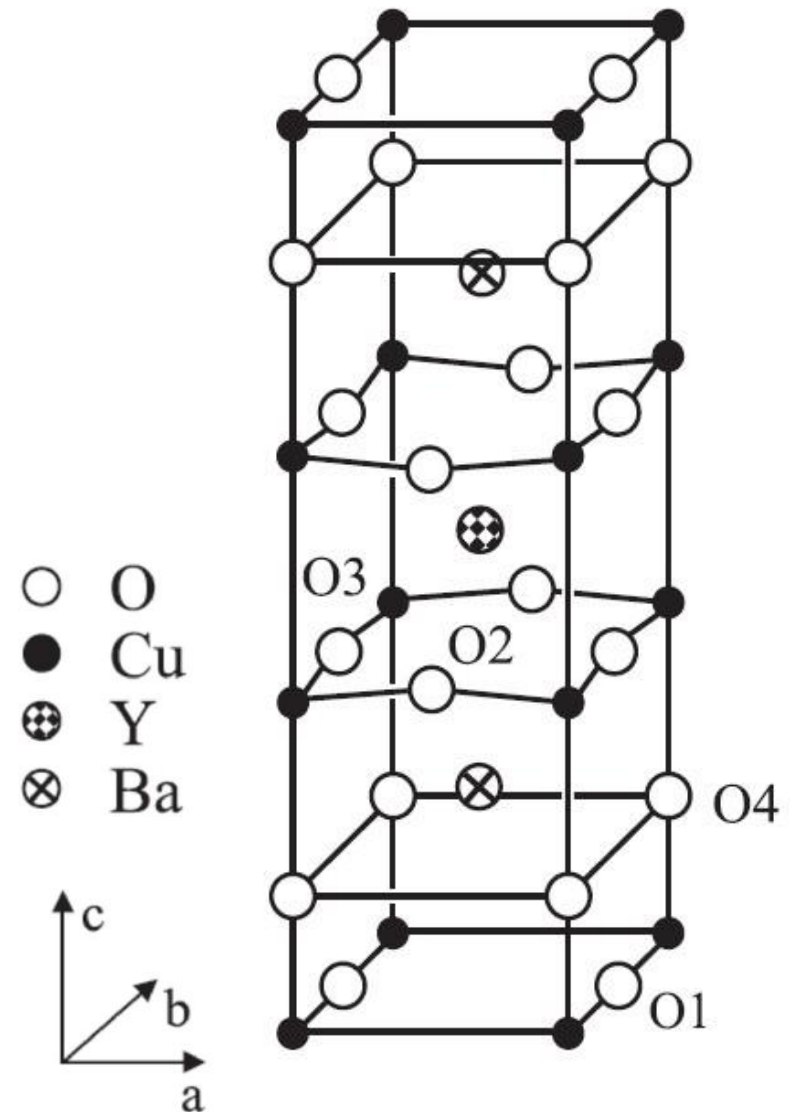
Perovskite structure of transition metal oxides

$\text{La}_{1-x}\text{Sr}_x\text{MnO}_3$, ferromagnet, $T_{\text{Curie}}=370\text{ K}$

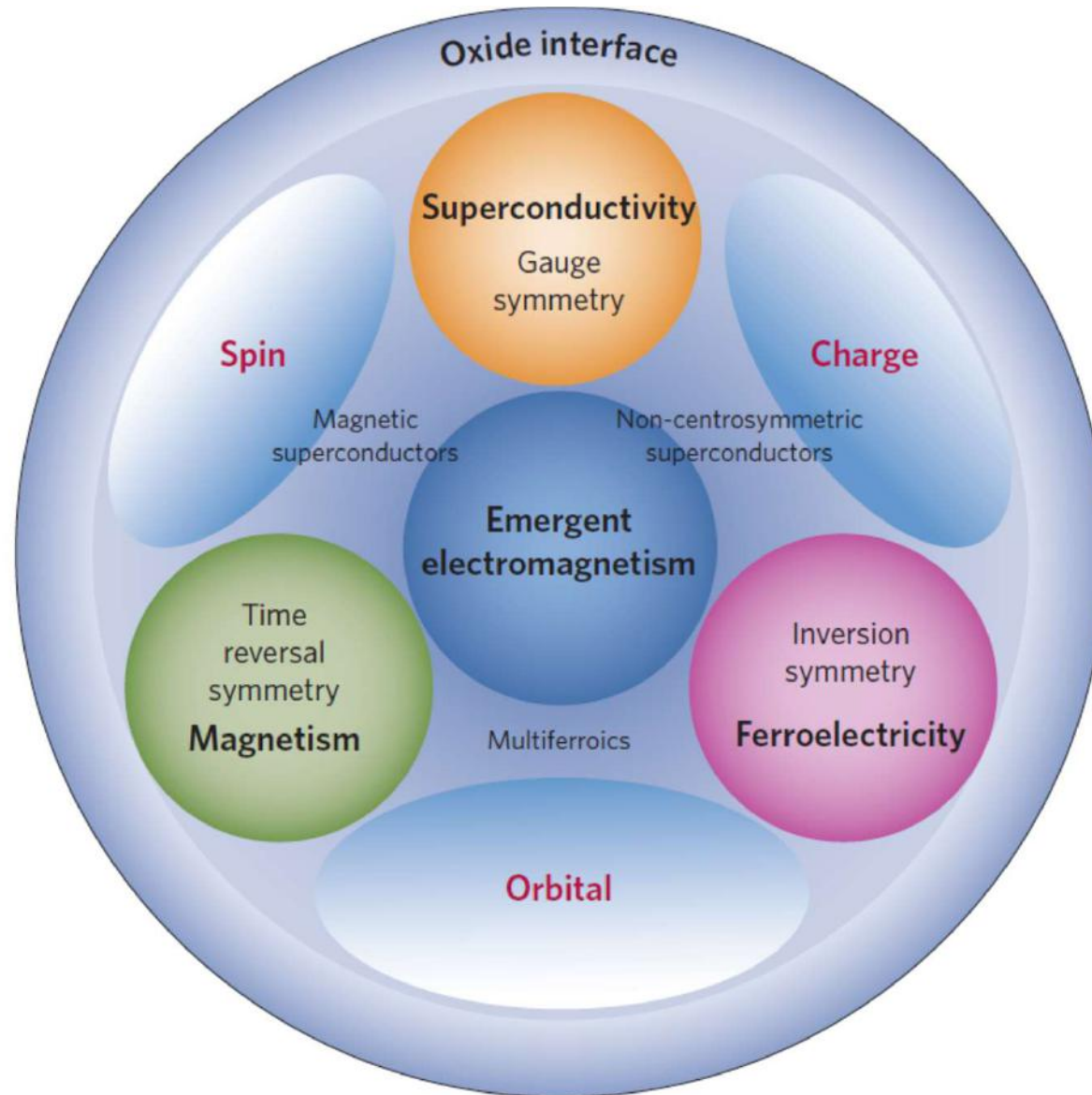


- perovskite structure is common to many transition metal oxides
- materials can be often combined epitaxially
- under favourable conditions, it is possible to grow multilayers with atomically sharp interfaces

$\text{YBa}_2\text{Cu}_3\text{O}_7$
 High temperature
 superconductor, $T_c=92\text{ K}$



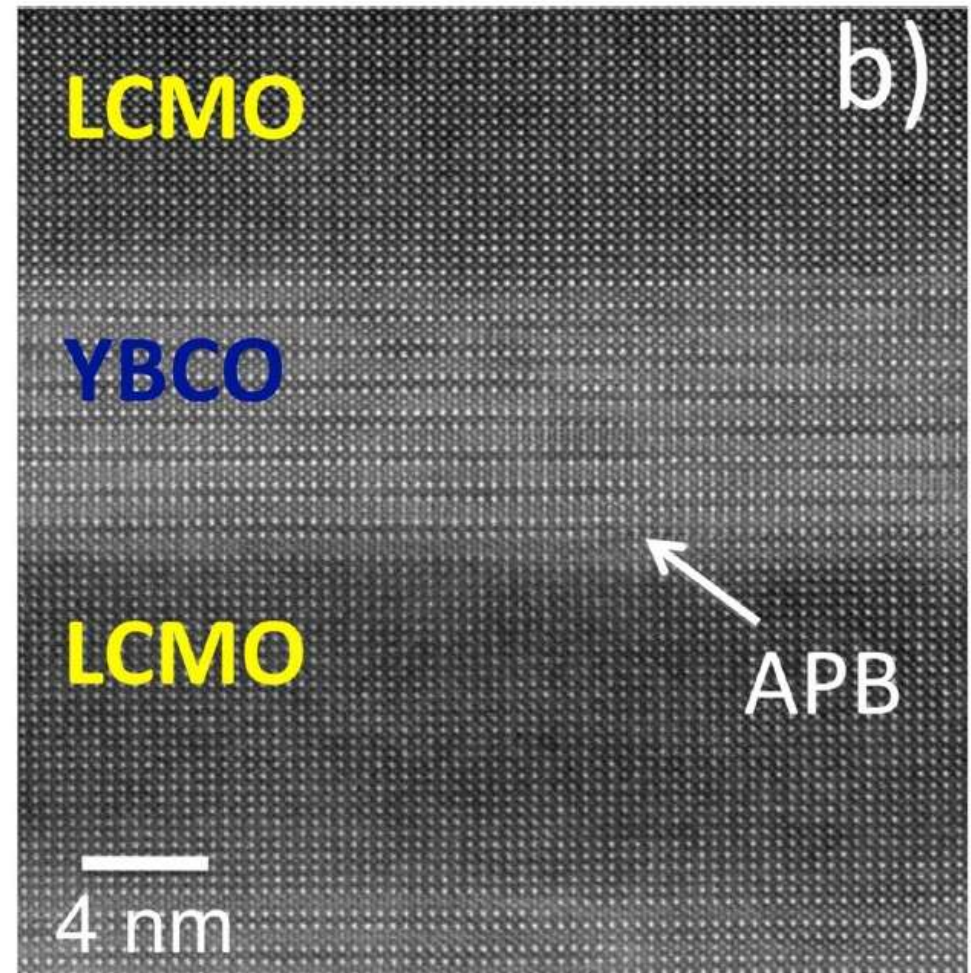
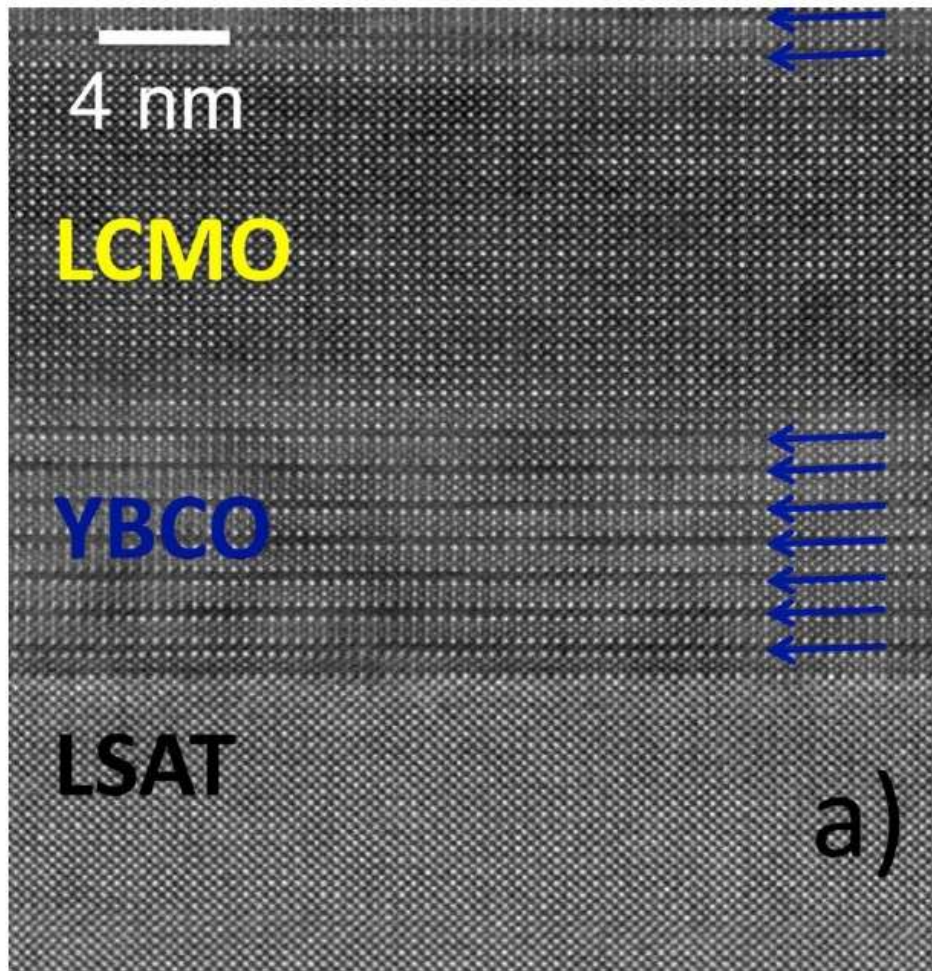
Potential of combining different electronic/magnetic orders at transition metal oxide interfaces



Multilayers of $\text{YBa}_2\text{Cu}_3\text{O}_7(n)/\text{La}_{0.7}\text{Ca}_{0.3}\text{MnO}_3(m)$

Competition between magnetism ($\text{La}_{0.7}\text{Ca}_{0.3}\text{MnO}_3$) and superconductivity ($\text{YBa}_2\text{Cu}_3\text{O}_7$)

Transmission electron microscope image with atomic resolution



Interfaces may have an important role

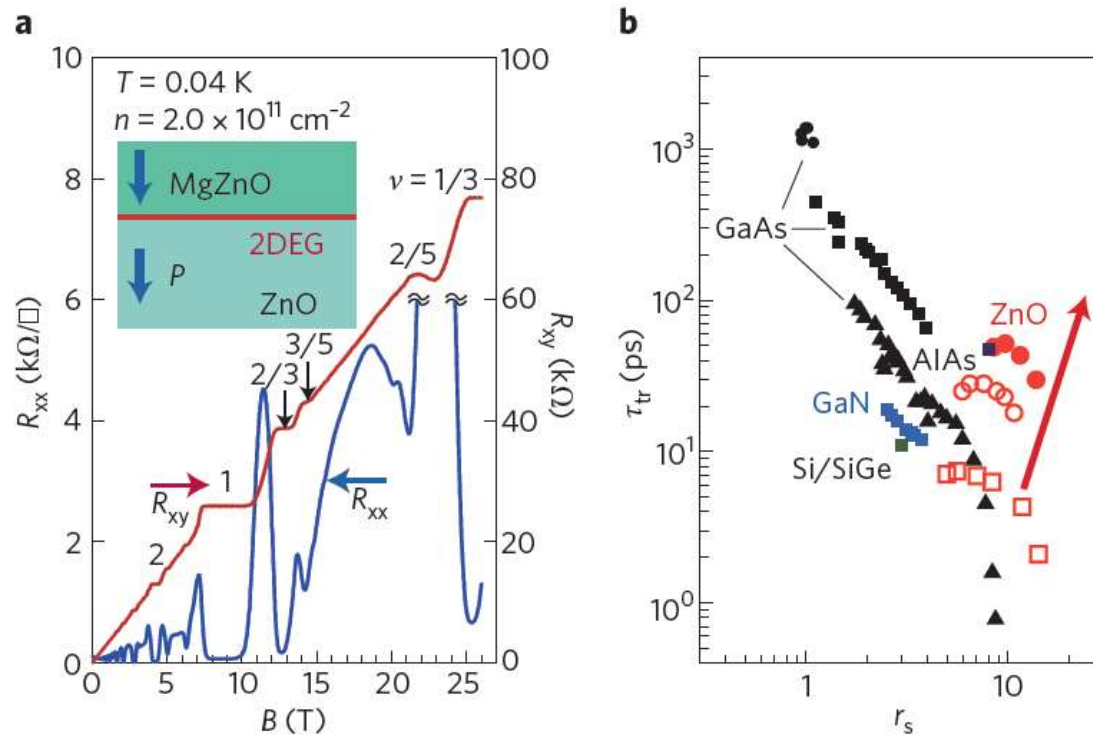
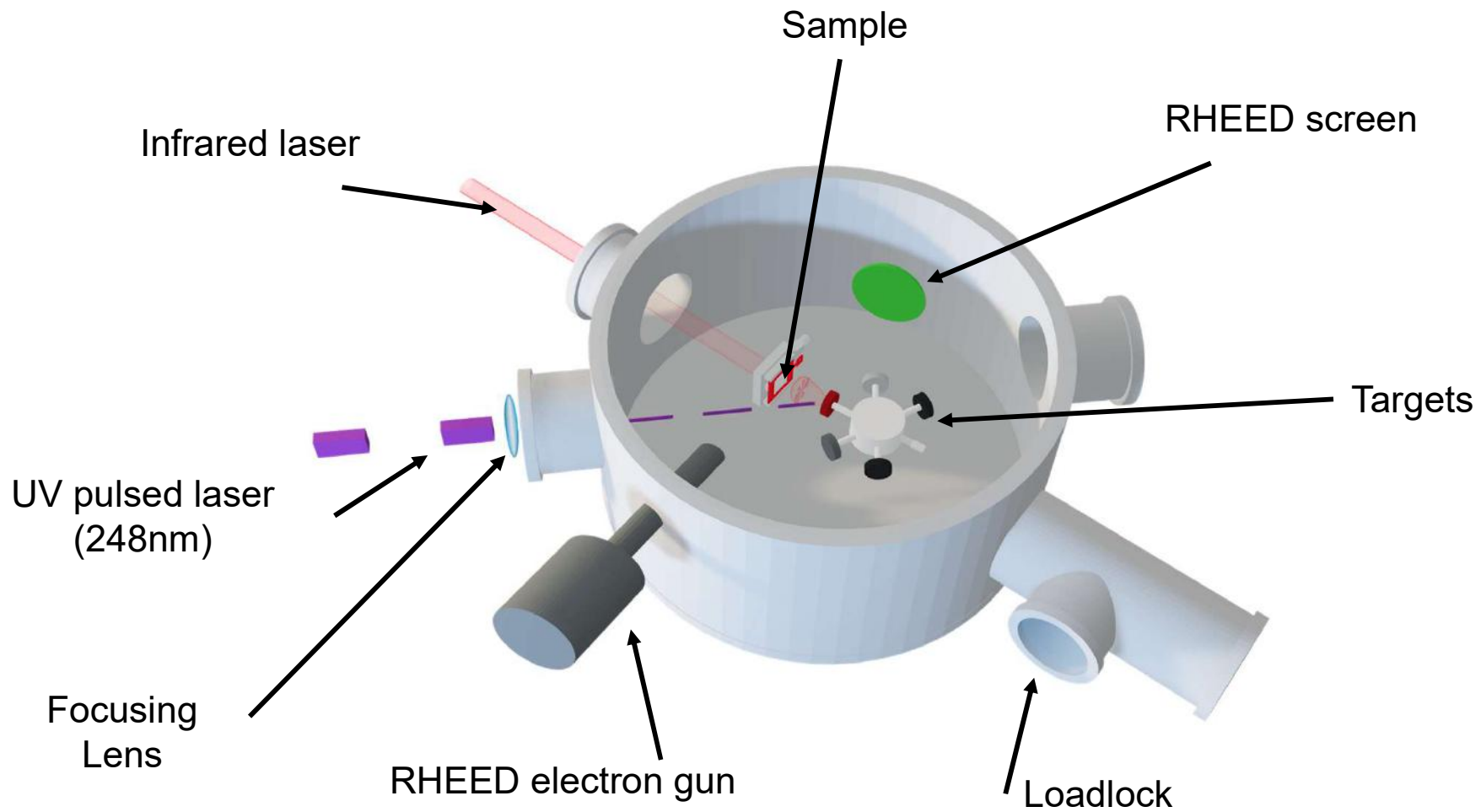


Figure 8 | Fractional quantum Hall effect in ZnO. **a**, Longitudinal resistance R_{xx} (blue) and Hall resistance R_{xy} (red) of a 2DEG formed at a MgZnO/ZnO interface. Inset: depicts a cross-sectional schematic of the heterostructure. **b**, Comparison of 2DEGs in various semiconductors as functions of the electron-electron interaction strength represented by the Wigner-Seitz radius r_s and transport scattering time τ_{tr} . Data are derived from Fig. 2 of ref. 81 except for the solid red circles, obtained for the sample shown in **a**. The arrow indicates the direction of progress in pursuing a regime of parameters in ZnO that are hard to access in other semiconductors. Panels adapted with permission from: **a**, ref. 83, © 2011 APS; **b**, ref. 81, © 2010 NPG.

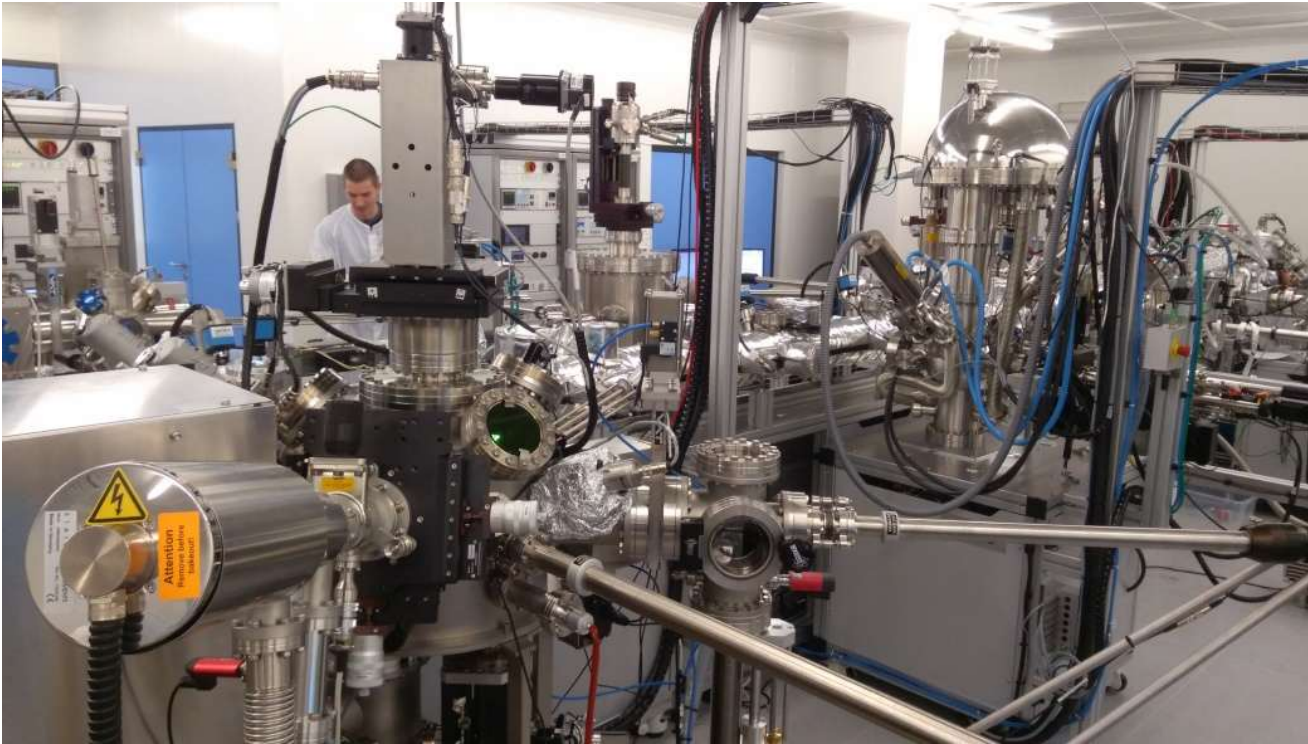
Herbert Kroemer: (Nobel price 2000): „Interface is THE device“

- 2D electron gas occurs at interface between MgZnO and ZnO
- mobility reaches up to very high numbers of $300,000 \text{ cm}^2 \text{ V}^{-1} \text{ s}^{-1}$ to observe fractional quantum Hall effect

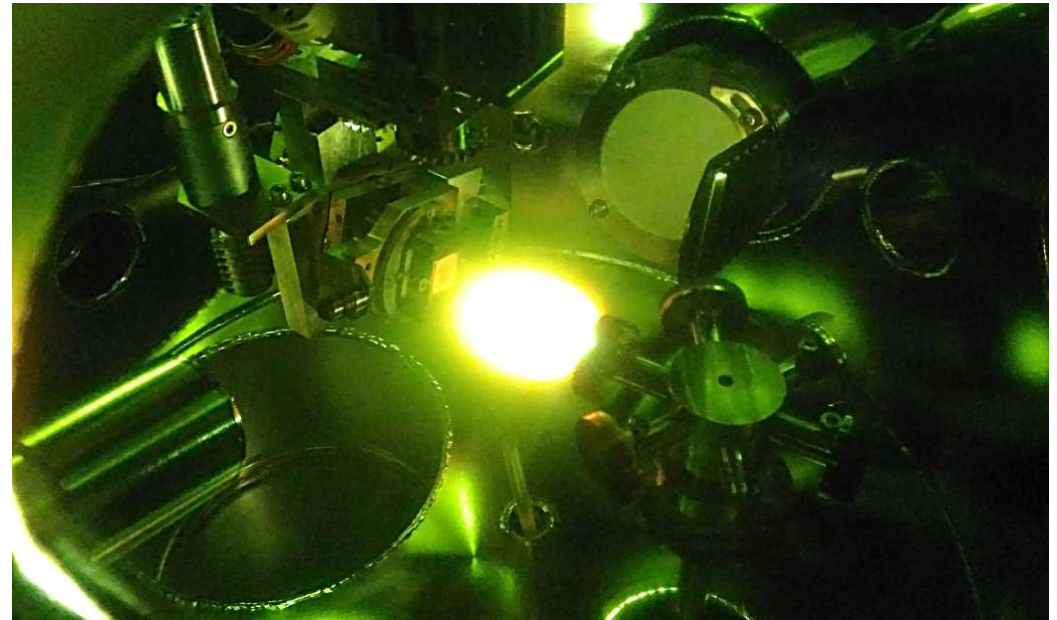
Scheme of the PLD chamber at CEITEC



PLD at CEITEC



- UHV conditions (10^{-8} mbar or better)
- in situ RHEED
- in situ ozone atmosphere
- connected to UHV cluster with additional deposition and analytical devices (XPS, ARPES, LEEM, LEED, STM)

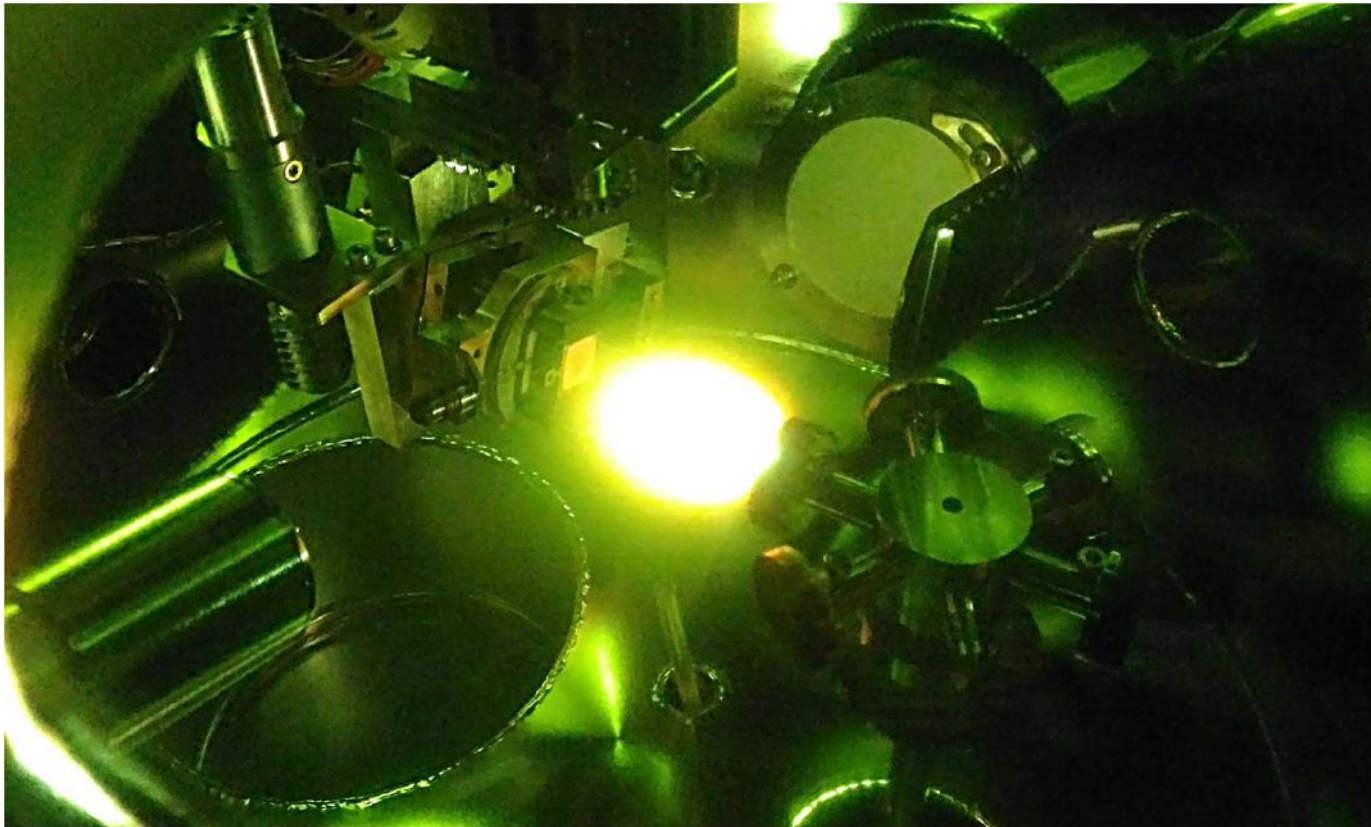


Materials we can deposit at CEITEC

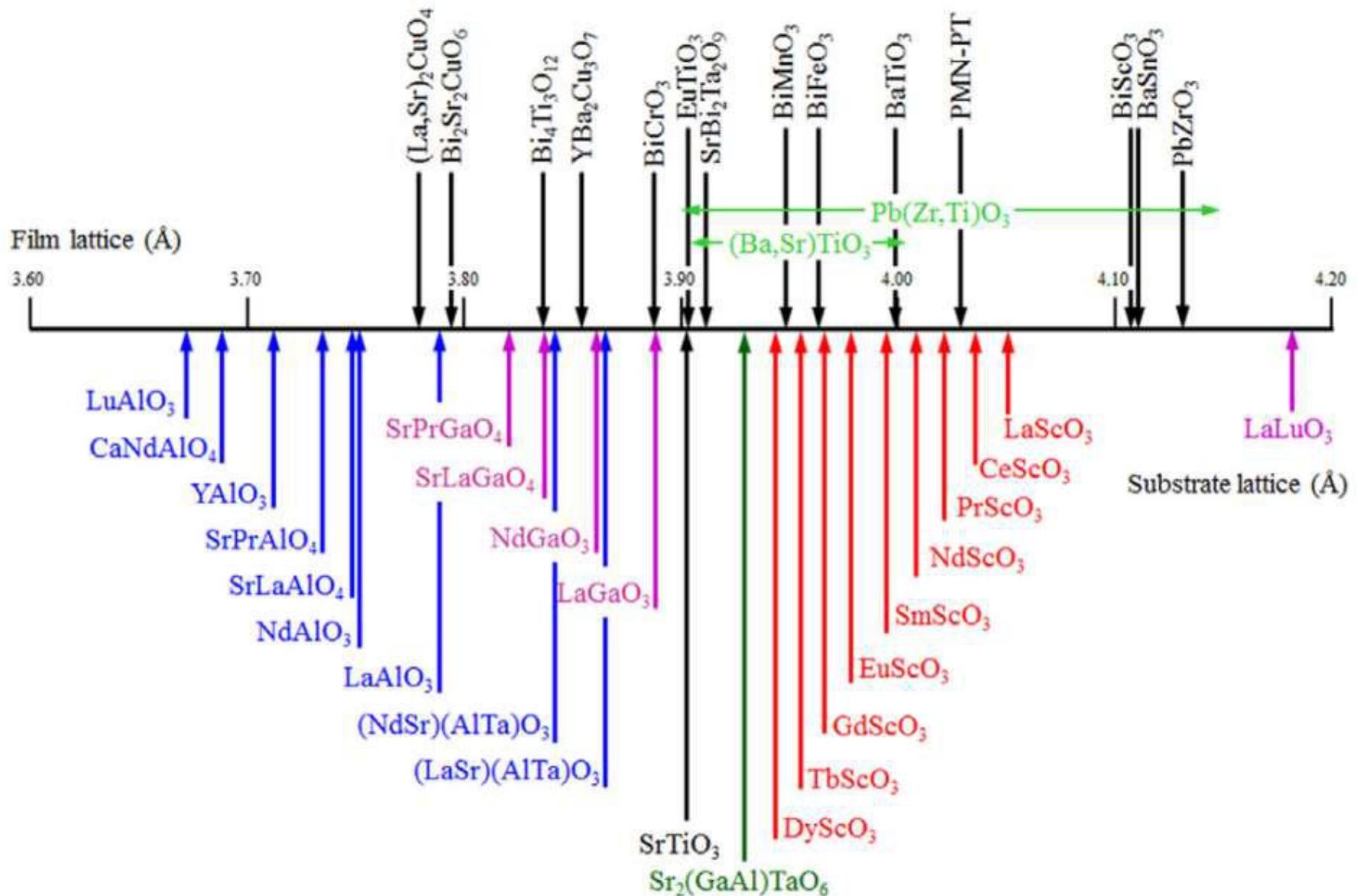
- LaFeO_3
 - $\text{La}_{0.33}\text{Sr}_{0.67}\text{FeO}_3$
 - $\text{La}_{0.5}\text{Sr}_{0.5}\text{FeO}_3$
 - $\text{La}_{0.6}\text{Sr}_{0.4}\text{FeO}_3$
 - SrFeO_3
- LaCoO_3
 - $\text{La}_{0.8}\text{Sr}_{0.2}\text{CoO}_3$
 - $\text{La}_{0.7}\text{Sr}_{0.3}\text{CoO}_3$
 - $\text{La}_{0.5}\text{Sr}_{0.5}\text{CoO}_3$
 - $\text{La}_{0.3}\text{Sr}_{0.7}\text{CoO}_3$
 - SrCoO_3
- LaCrO_3
 - SrRuO_3
 - SrTiO_3
 - SrTiO_3 0.7% Nb doped
 - SrTiO_3 1.4% Nb doped
 - LaAlO_3
 - $\text{La}_{0.67}\text{Sr}_{0.33}\text{MnO}_3$
 - $\text{YBa}_2\text{Cu}_3\text{O}_7$

Typical deposition conditions for growth of transition metal oxides

- 0.01-0.5 mbar oxygen pressure
- 500C – 800C substrate temperature (typical), but may go between 30-1200 deg C
- 1 J.cm⁻² – 3 J.cm⁻² laser fluency
- 1 Hz -10 Hz laser frequency
- from target to substrate distance of about 5 cm



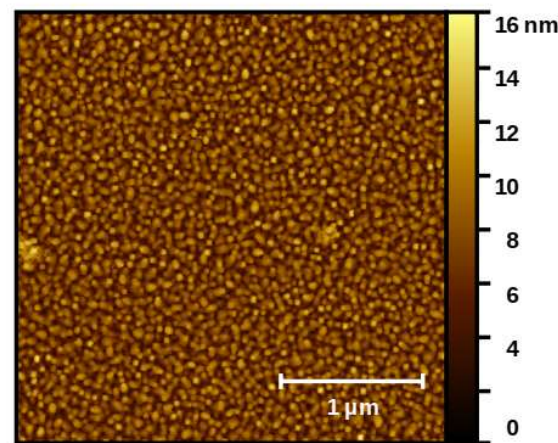
Lattice matching to substrates



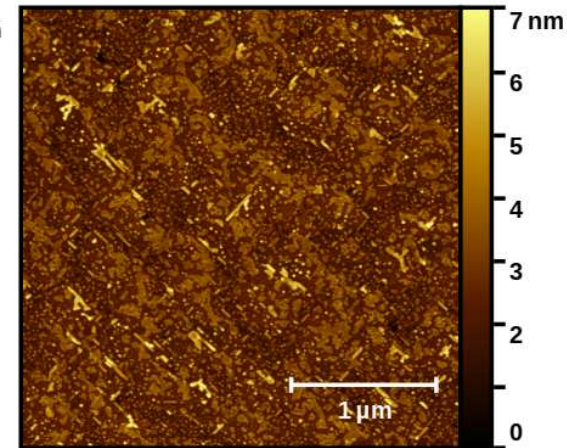
An example of a single layer $\text{La}_{0.7}\text{Sr}_{0.3}\text{MnO}_3$ (J. Klimek)

| | gas | Pressure (mbar) | No pulses | Deg C | Fluency [J/cm ²] |
|-------|------|--------------------|--------------|-------|---------------------------------|
| JK001 | LSAT | O ₂ | 10 | 730 | 2 |
| JK004 | LSAT | O ₃ | 5 | 730 | 2 |
| JK005 | LSAT | O ₃ | 5 | 730 | 2.5 |
| JK008 | LSAT | O ₃ | 5 | 730 | 2.5 |

$\sigma_{\text{RMS}} = 2.1 \text{ nm}$
rough sample
0.3 mbar in O₂

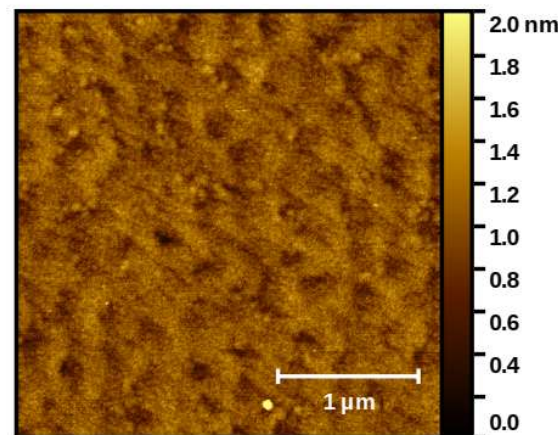


(a) JK001 ($\sigma = 2.1 \text{ nm}$)

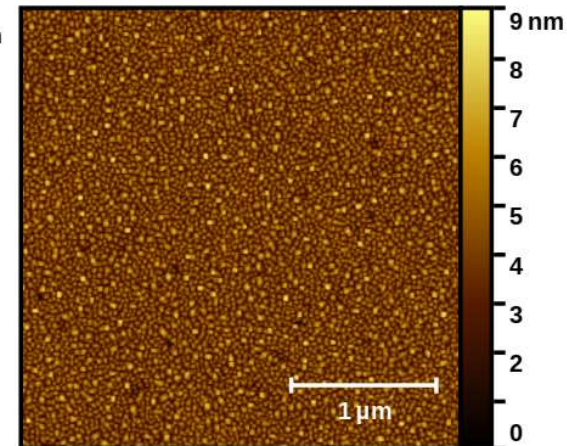


(b) JK004 ($\sigma = 0.93 \text{ nm}$)

$\sigma_{\text{RMS}} = 0.2 \text{ nm}$
(below 1 ML)
atomically flat film
0.1 mbar in O₃

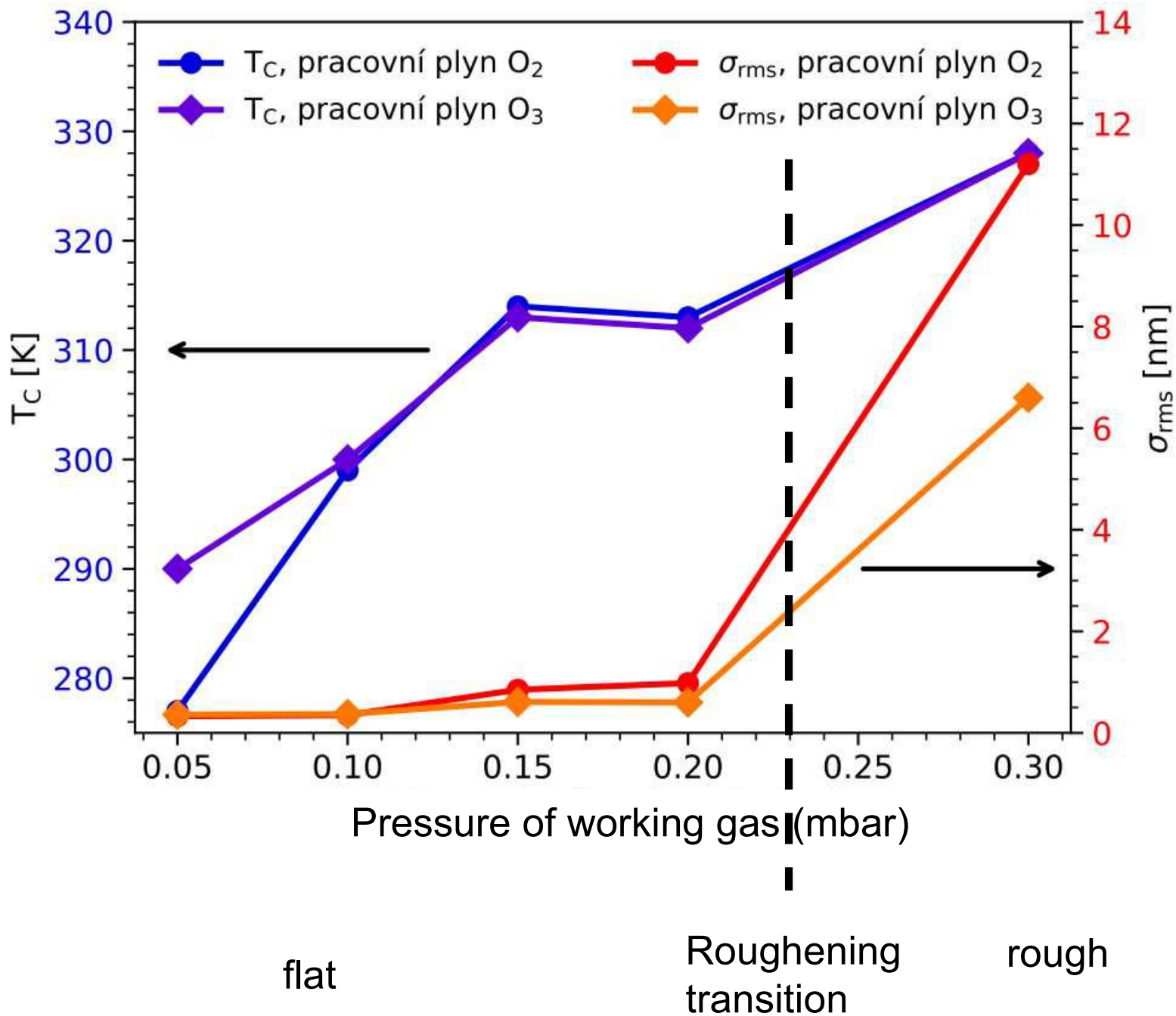


(c) JK005 ($\sigma = 0.2 \text{ nm}$)



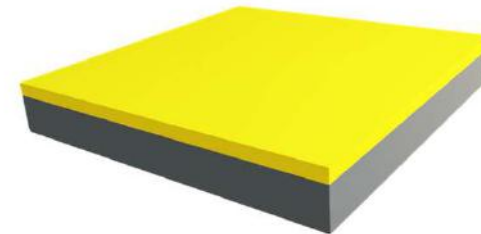
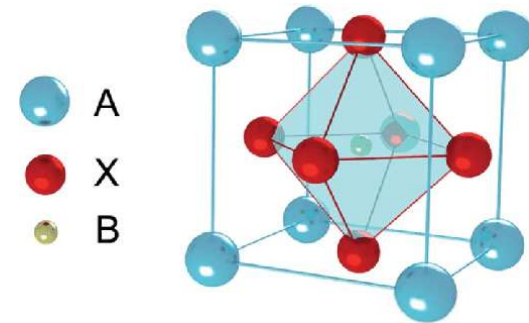
(d) JK008 ($\sigma = 1.15 \text{ nm}$)

Roughening transition in $\text{La}_{0.7}\text{Sr}_{0.3}\text{MnO}_3$ (J. Klimek)



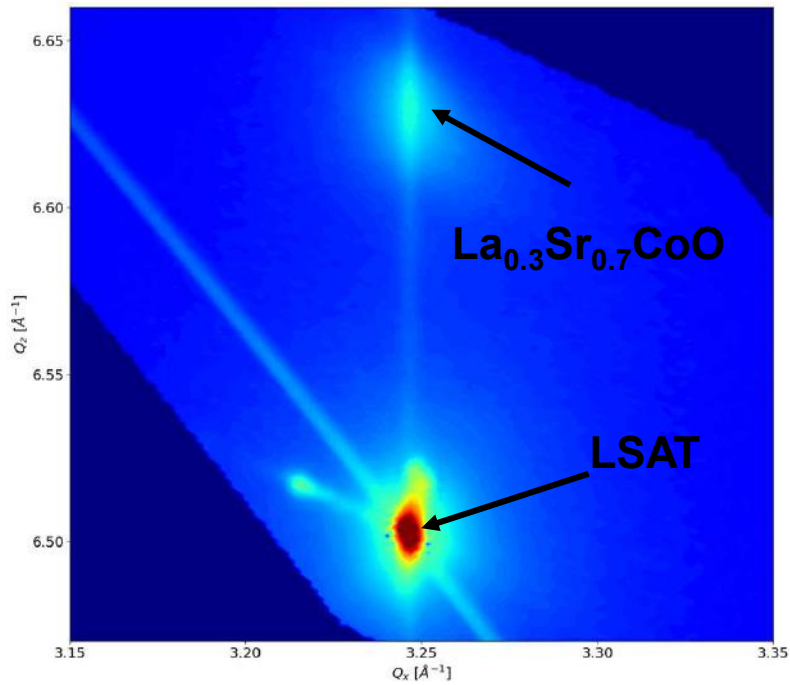
$\text{La}_{0.3}\text{Sr}_{0.7}\text{CoO}_3/\text{LSAT}$

- Ferromagnet with bulk Curie temperature of about 245K (280K*)
- Cubic perovskite structure with lattice parameter $a=3.824 \text{ \AA}^*$
- LSAT substrate has a cubic lattice with a lattice parameter of 3.868 \AA
- Samples are annealed at 400 C in ozone atmosphere for 3 hours to fully oxidize film.

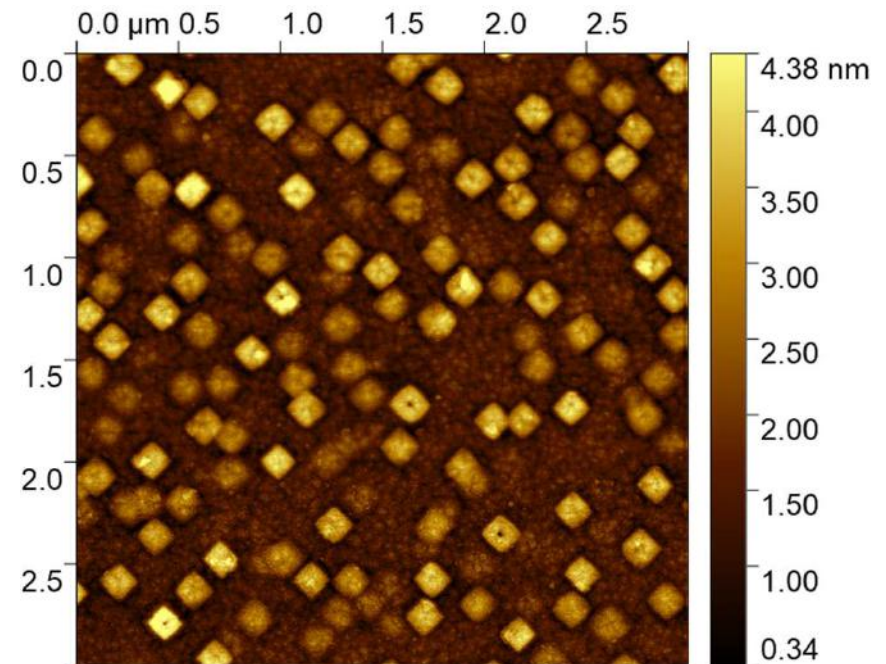


*M. Chennabasappa, E. Petit, and O. Toulemonde, Ceram. Int. 46, 6067 (2020)

La_{0.3}Sr_{0.7}CoO₃/LSAT structural characterization

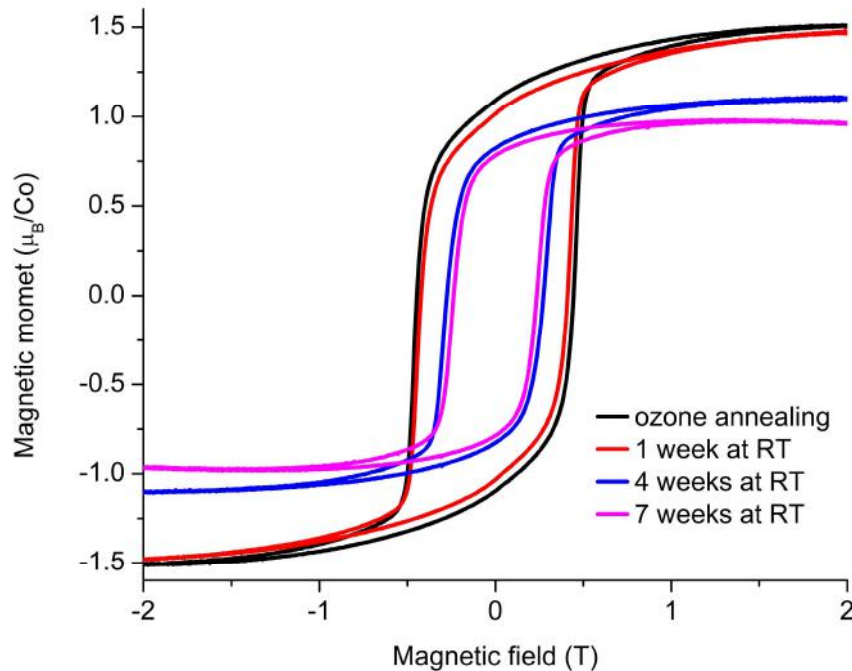


Reciprocal space map of La_{0.3}Sr_{0.7}CoO₃ film grown on LSAT in vicinity of 204 reciprocal lattice point

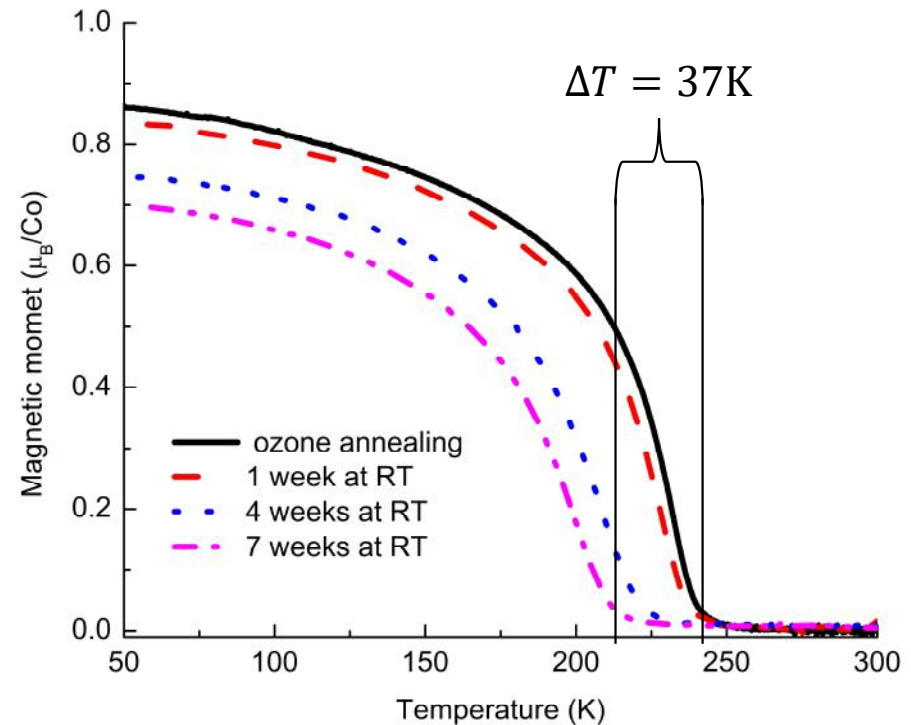


AFM image of the sample (27 nm) surface with mean roughness of 0.75 nm

Evolution of $\text{La}_{0.3}\text{Sr}_{0.7}\text{CoO}_3$ magnetic properties at room temperature in time

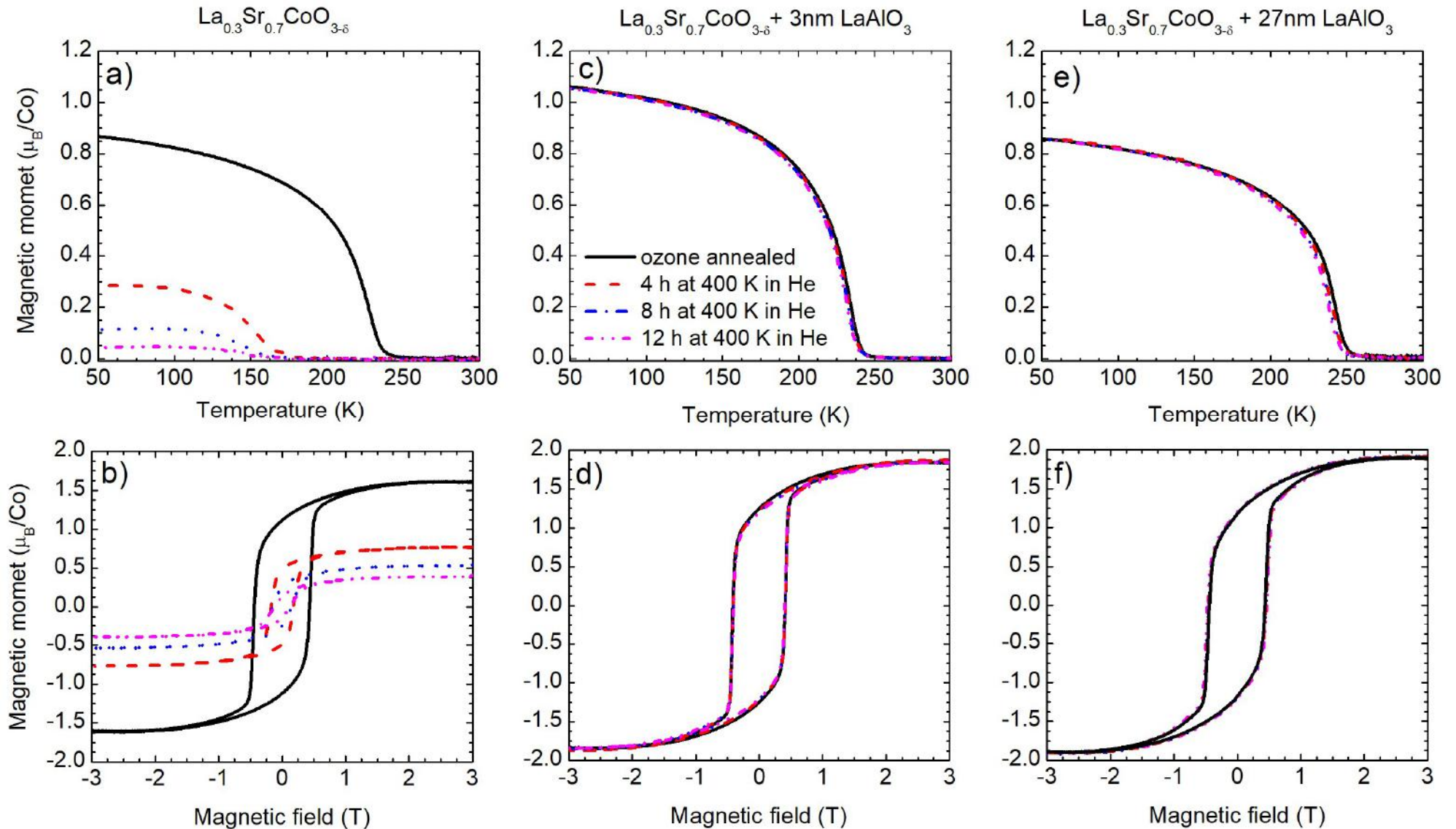


Magnetic hysteresis loop measured at 50K

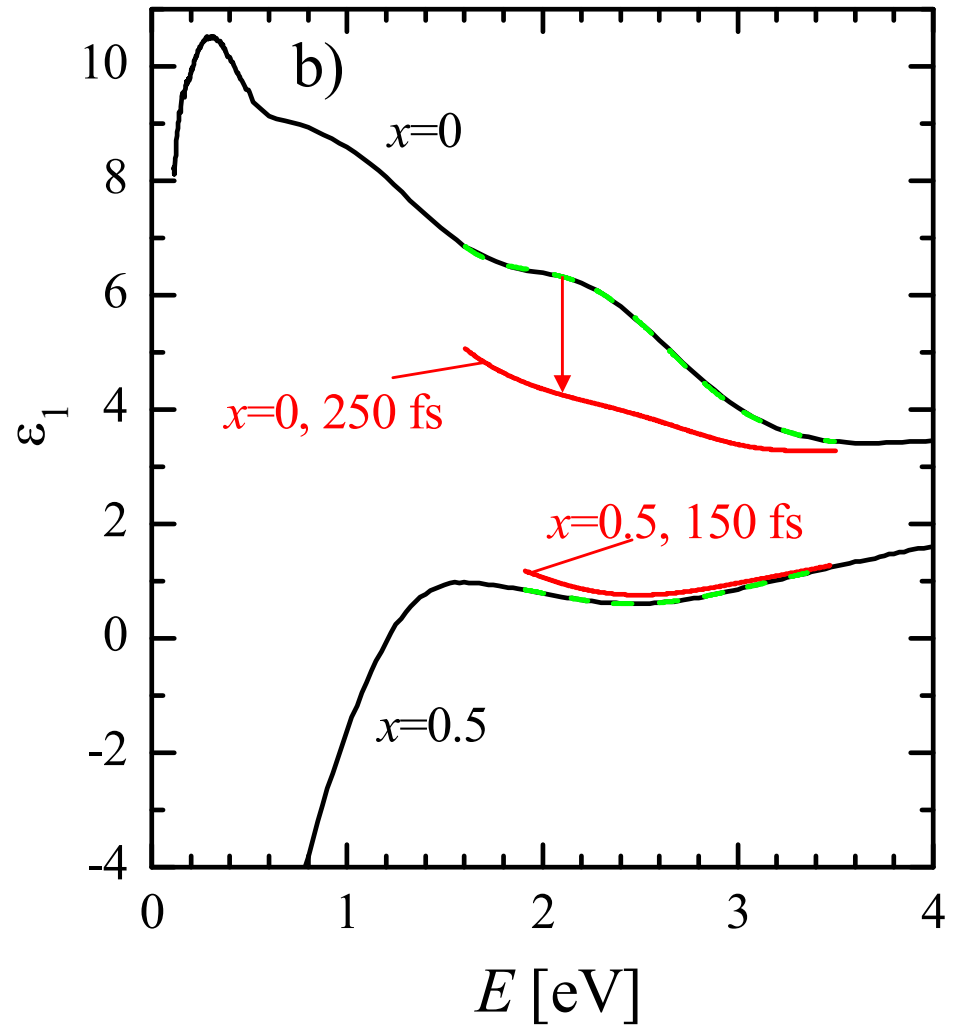
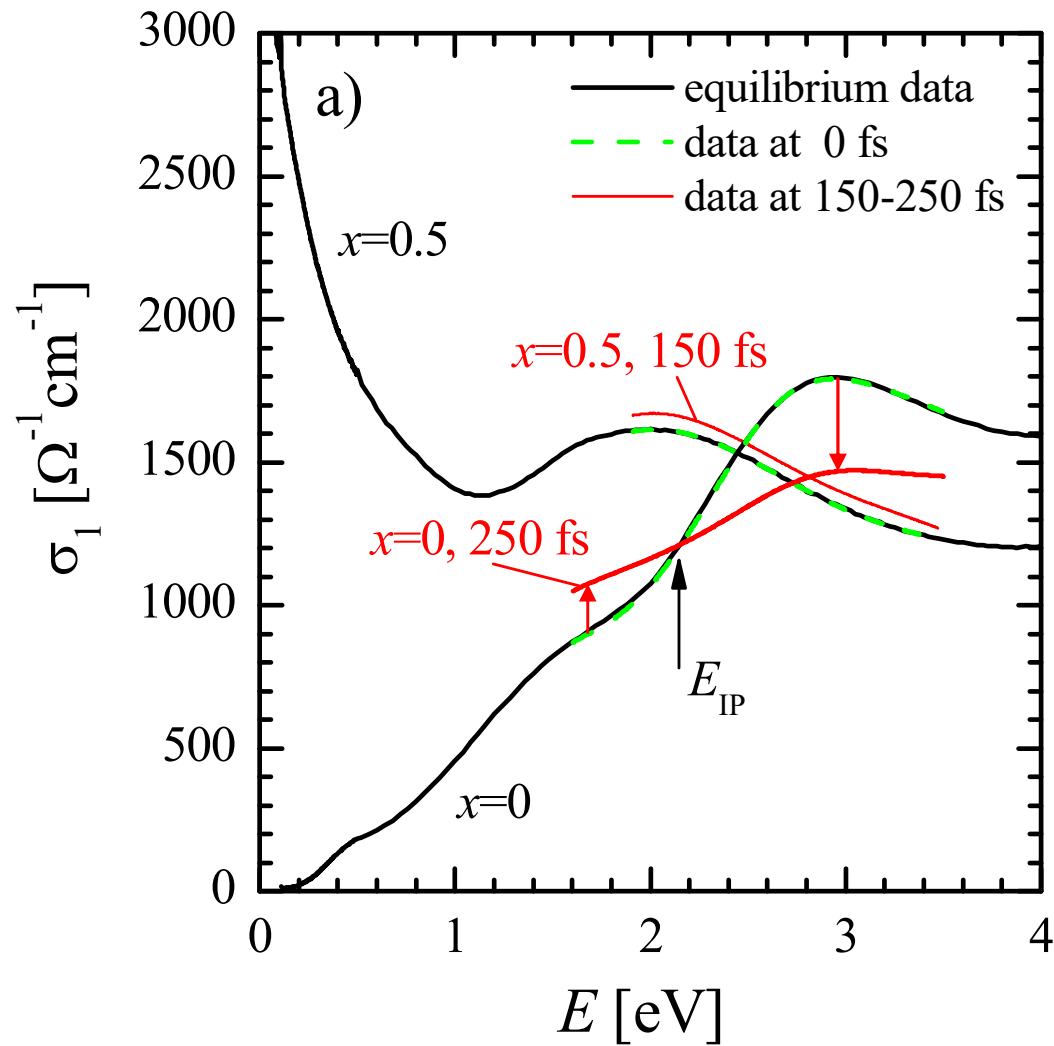


Magnetic moment vs temperature at magnetic field of 10 mT

Stabilization of oxygen in $\text{La}_{0.3}\text{Sr}_{0.7}\text{CoO}_{3}$ by only 3nm thin LaAlO_3 capping layer

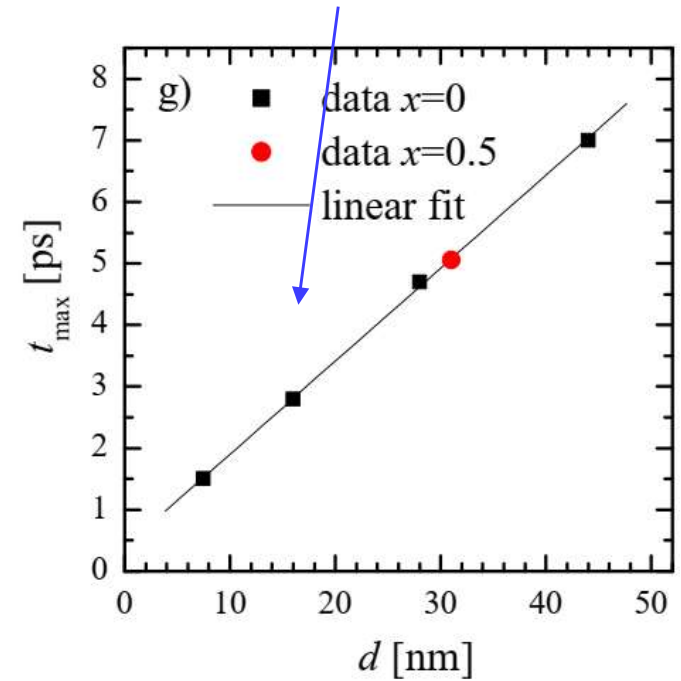
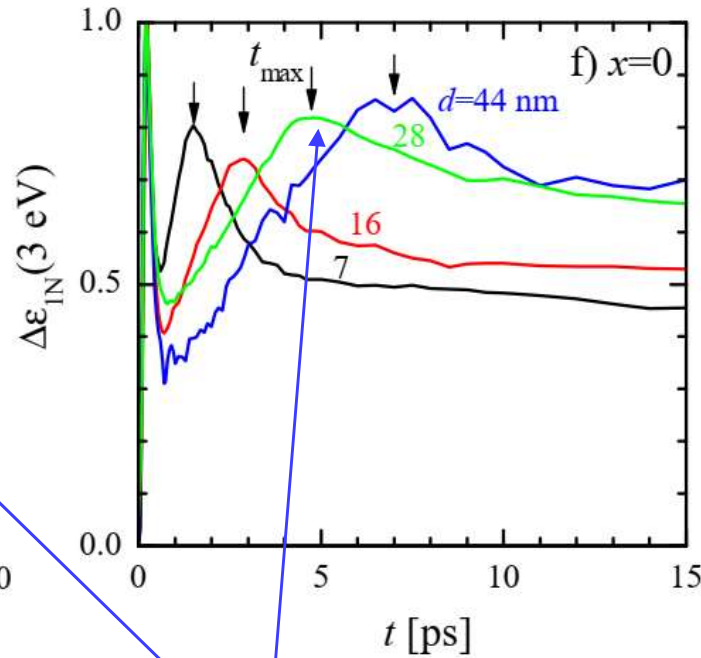
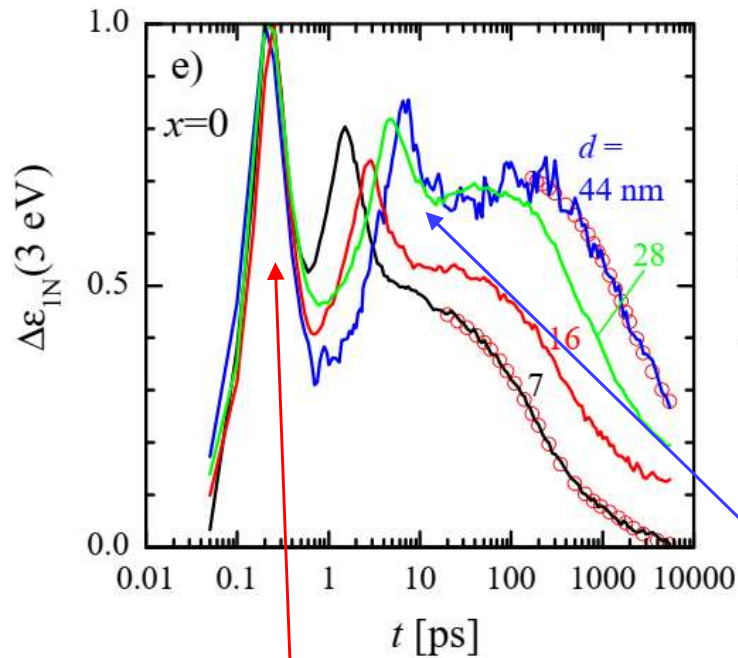


Pump-probe response of $\text{La}_{1-x}\text{Sr}_x\text{CoO}_3$



Measurements of samples with **various thickness**

Its delay is linear with thickness



The first peak is thickness independent
–**BULK** phenomenon

Secondary transient peak is dependent
on film thickness - **PROPAGATION** of a
pulse or wave.

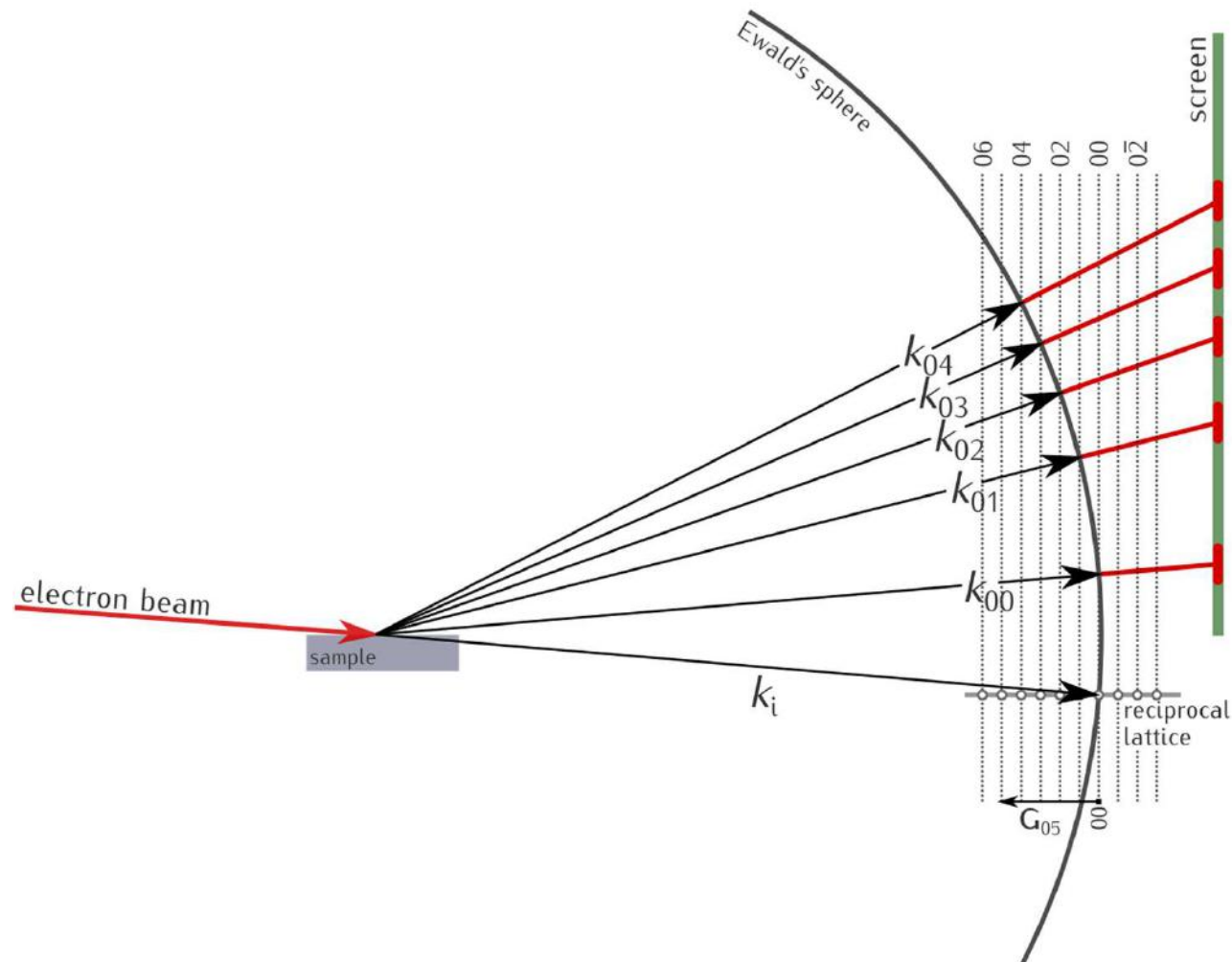
Assuming the secondary peak delay corresponds to the propagation of
the pulse between surface and the interface, we get the velocity
 $v=5.7\pm0.5$ nm/ps

RHEED - Ewald construction

Ewald construction:

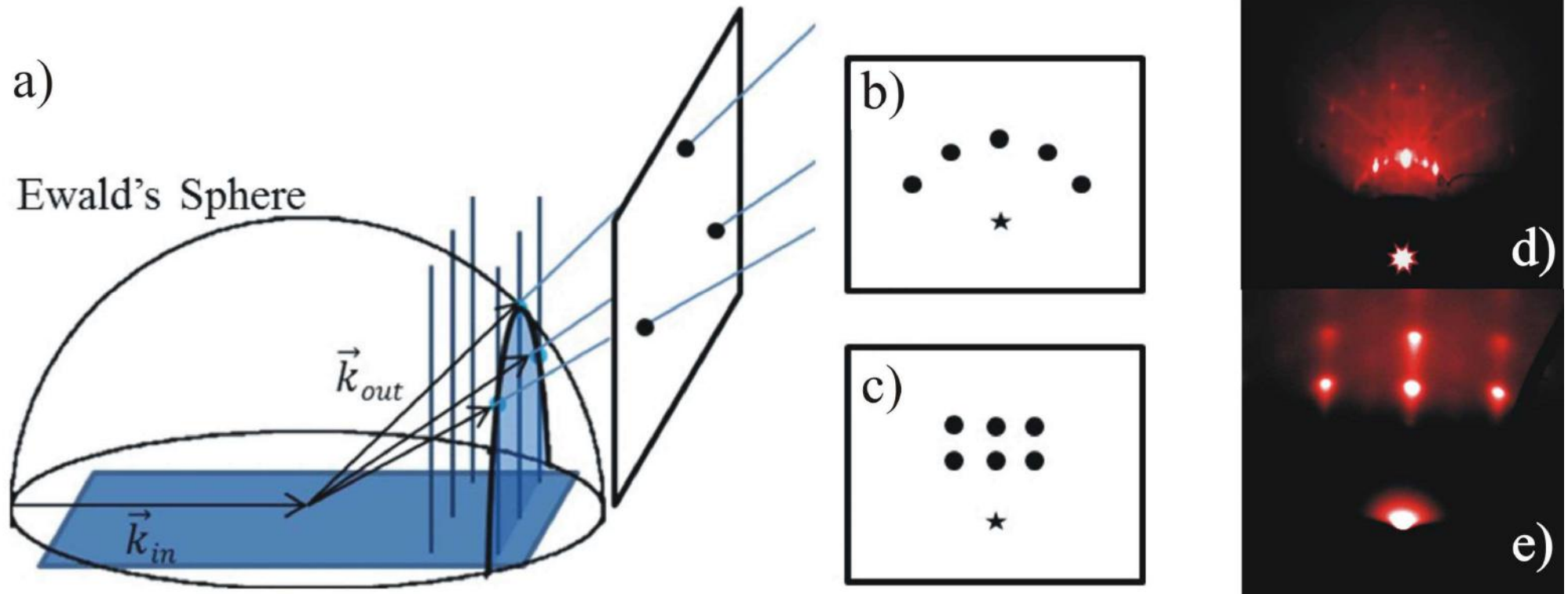
- circle (or sphere in 3D) represents the law of conservation of energy for elastic scattered beams \mathbf{k}_{hl} of the incident beam \mathbf{k}_i , $abs(\mathbf{k}_{hl})=abs(\mathbf{k}_i)$
- since RHEED occurs only at surface monolayer, there are no diffraction conditions for the direction perpendicular to the surface. Reciprocal lattice of surface is formed by a system of rods perpendicular to the surface.
- The projections of the two vectors \mathbf{k}_{hl} and \mathbf{k}_i on the sample surface differ by the scattered vector \mathbf{G}_{hl}

$$\mathbf{G}_{hl} = \mathbf{k}_{hl}^{\parallel} - \mathbf{k}_i^{\parallel}$$



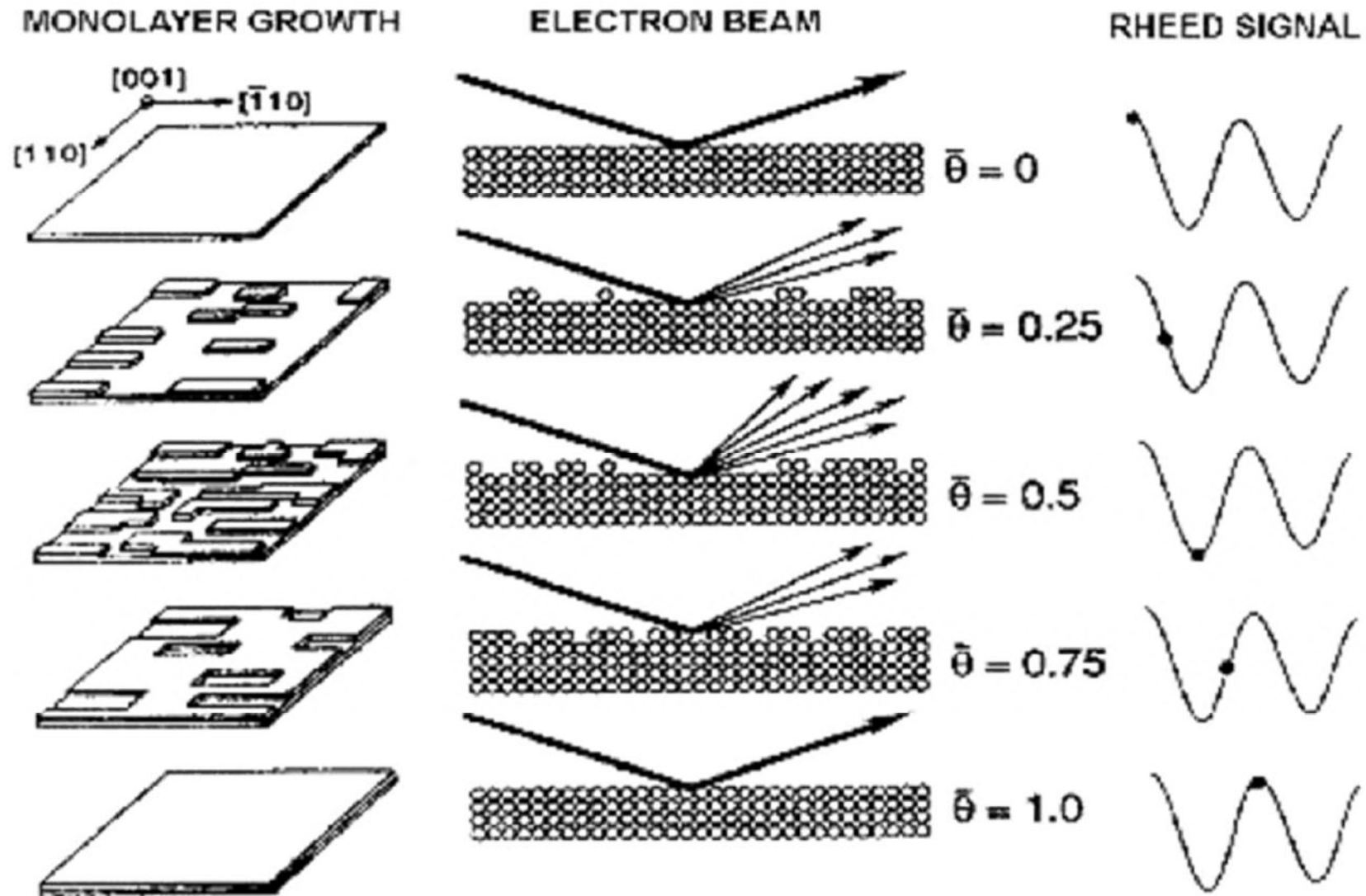
RHEED - Ewald construction

PLD group Paul Scherrer Institute, Fluri et al, (2018)

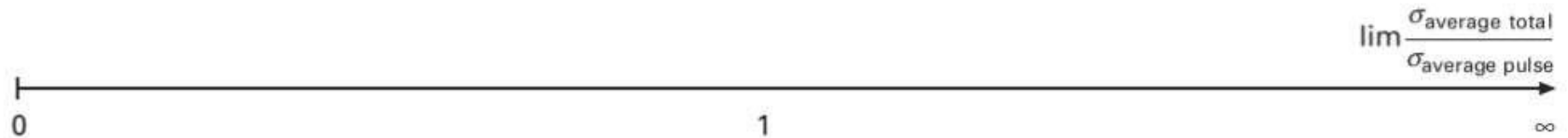
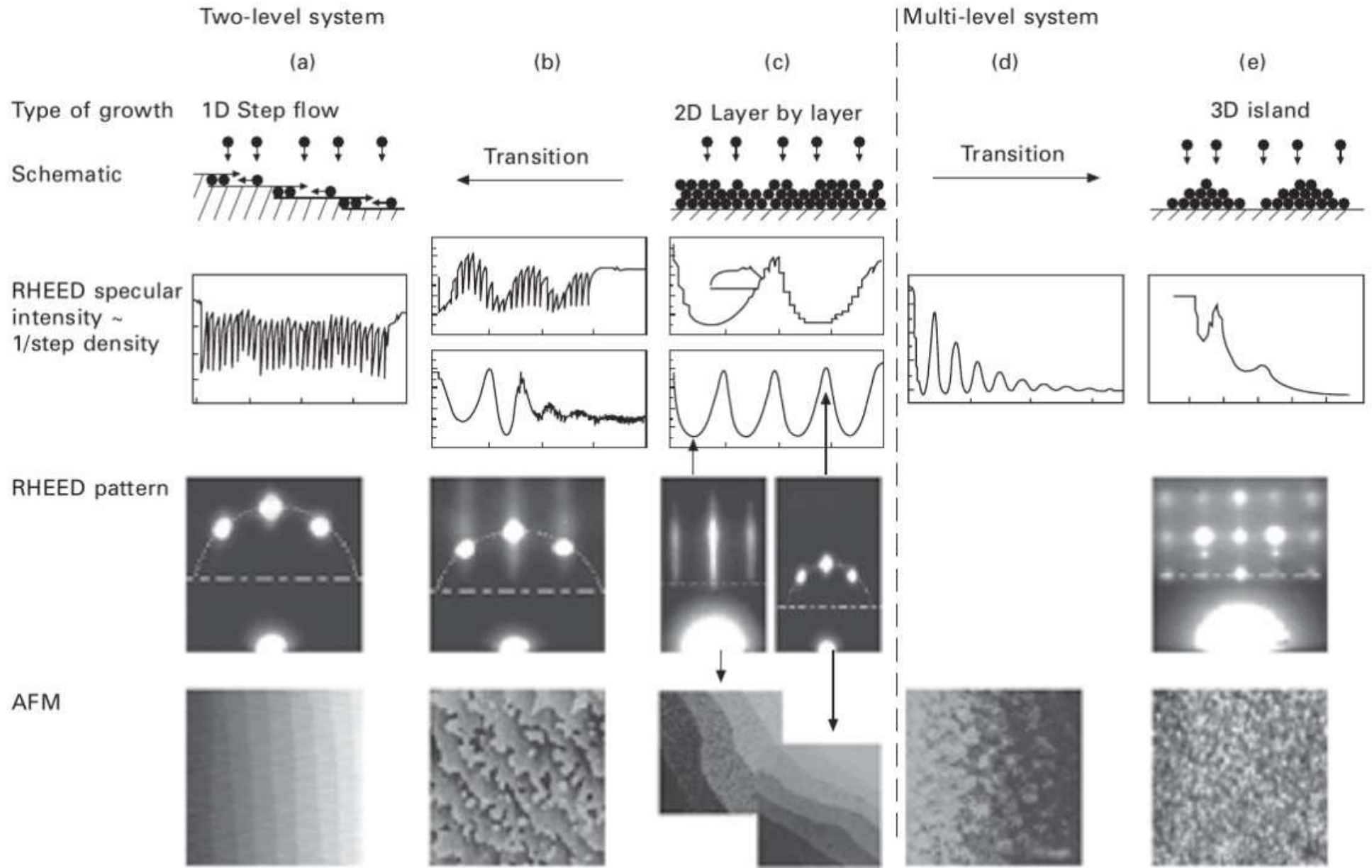


- (a) In three dimension, there the energy conservation condition gives rise to Ewald sphere
- (b) diffraction of an atomically flat sample corresponds to the diffraction points on a circle
- (c) on a surface formed by islands, the electrons go through them and scatter as in 3d – periodic pattern is formed

Evolution of RHEED signal during the layer by layer growth

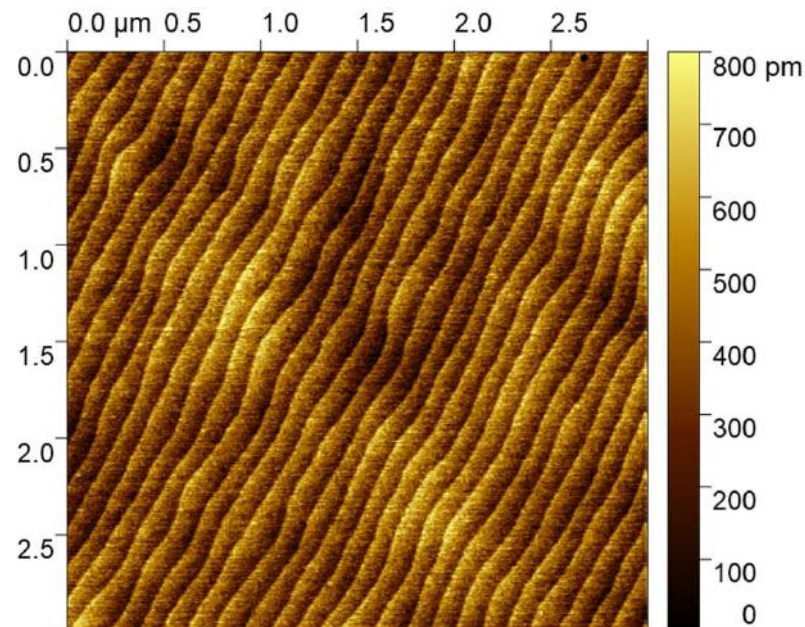
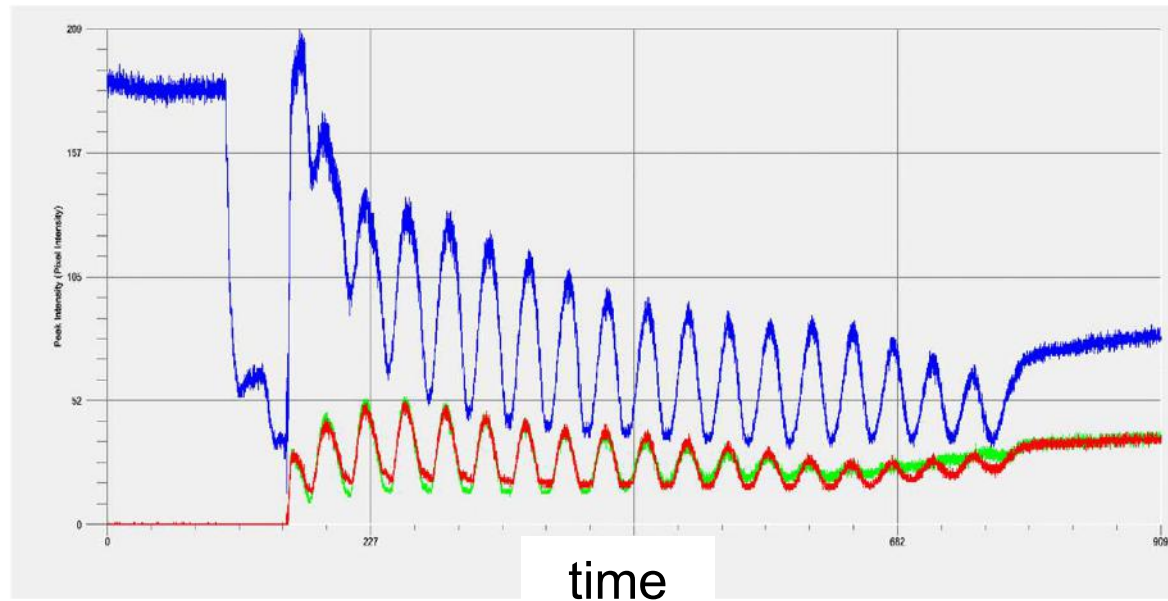


Examples of RHEED pictures



RHEED oscillations during growth of LaFeO_3 layer

RHEED oscillations: 20 monolayers of LaFeO_3

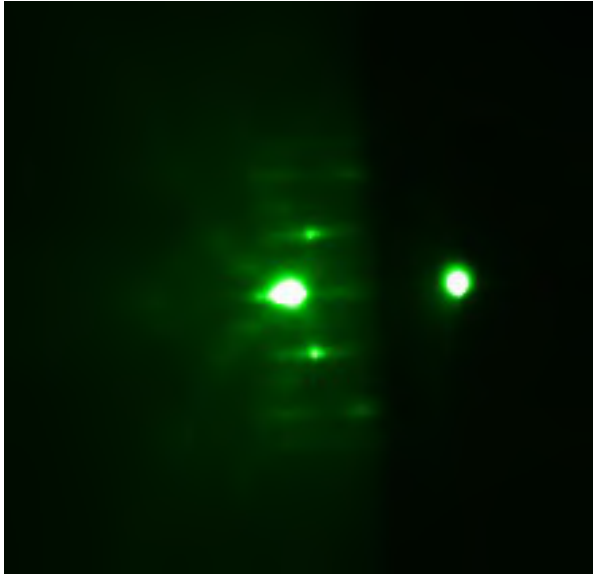


**Atomic
flatness
preserved!**

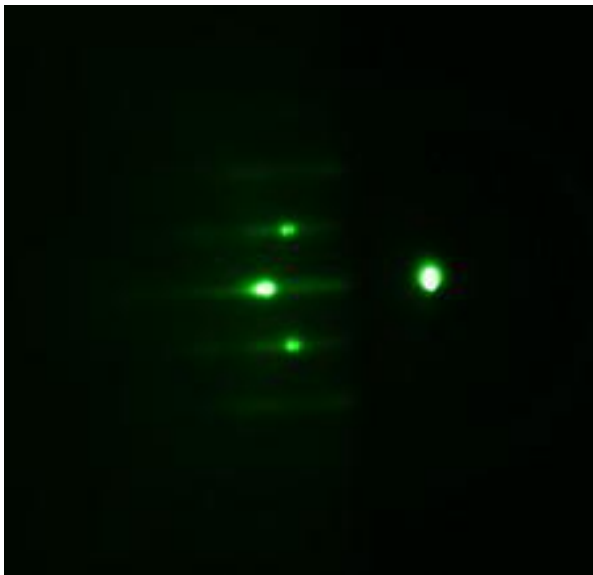
Deposition of $[\text{LFO}_1+\text{STO}_1]_{10}$ superlattice

RHEED pattern

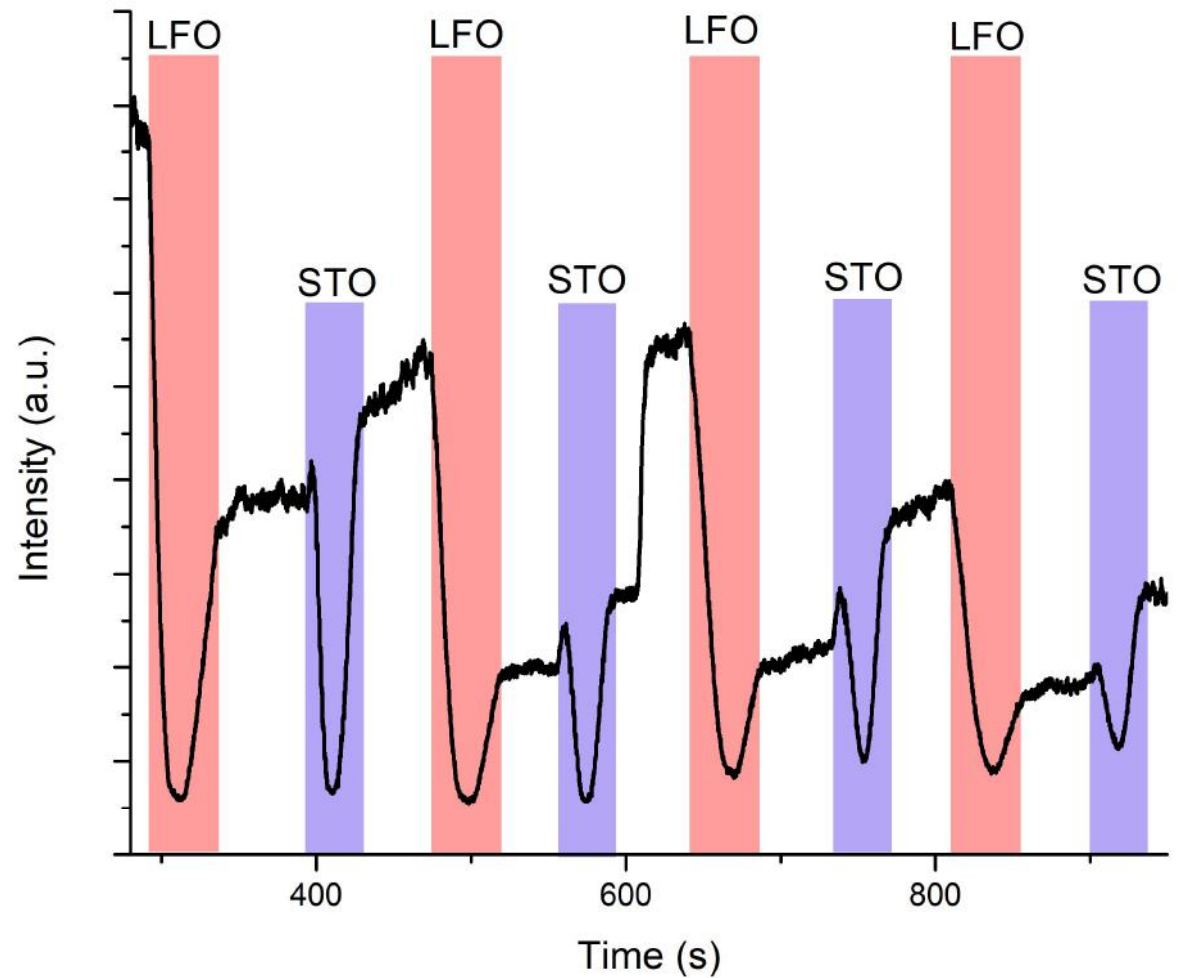
Before deposition



After deposition



RHEED intensity evolution during deposition



Superlattices $[\text{LFO}_1+\text{STO}_1]_{10}$

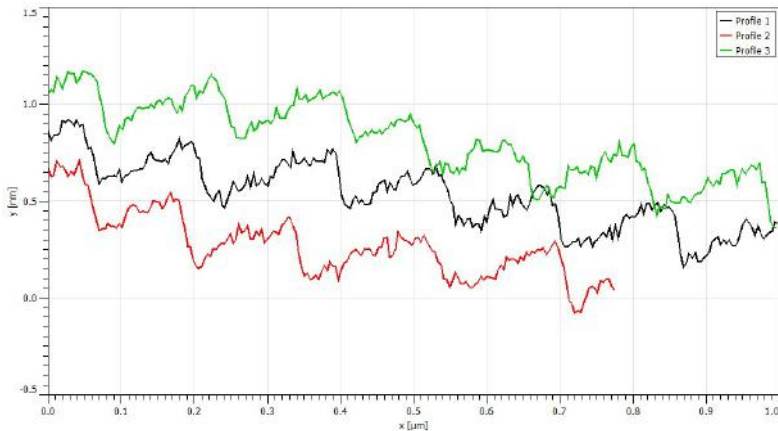
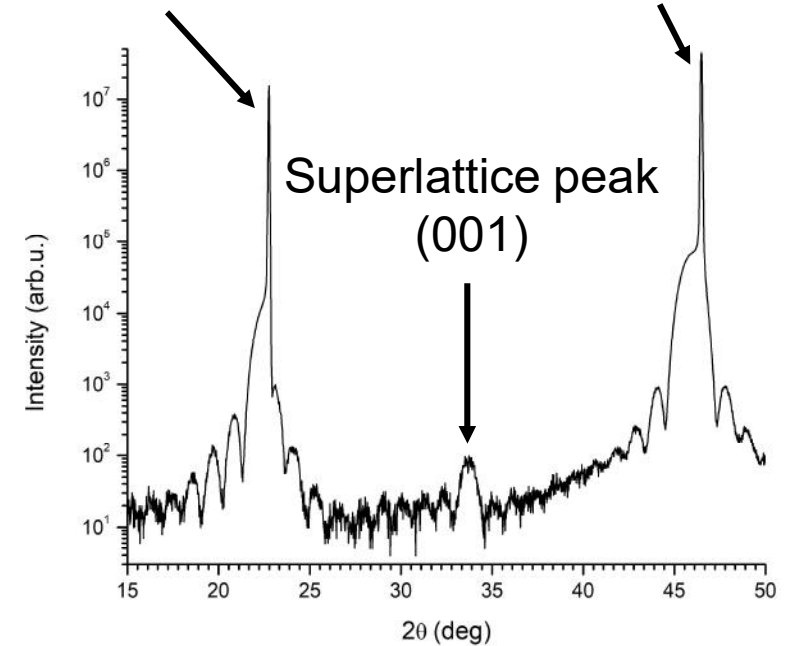
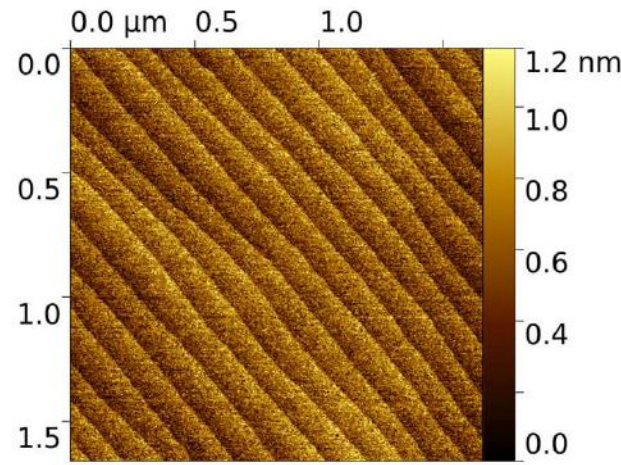
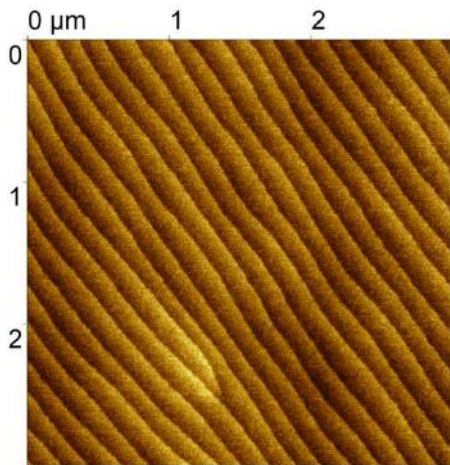
AFM image of the surface

X-ray diffraction of $[\text{LFO}_1+\text{STO}_1]_{10}$ superlattice

STO (001) STO (002)

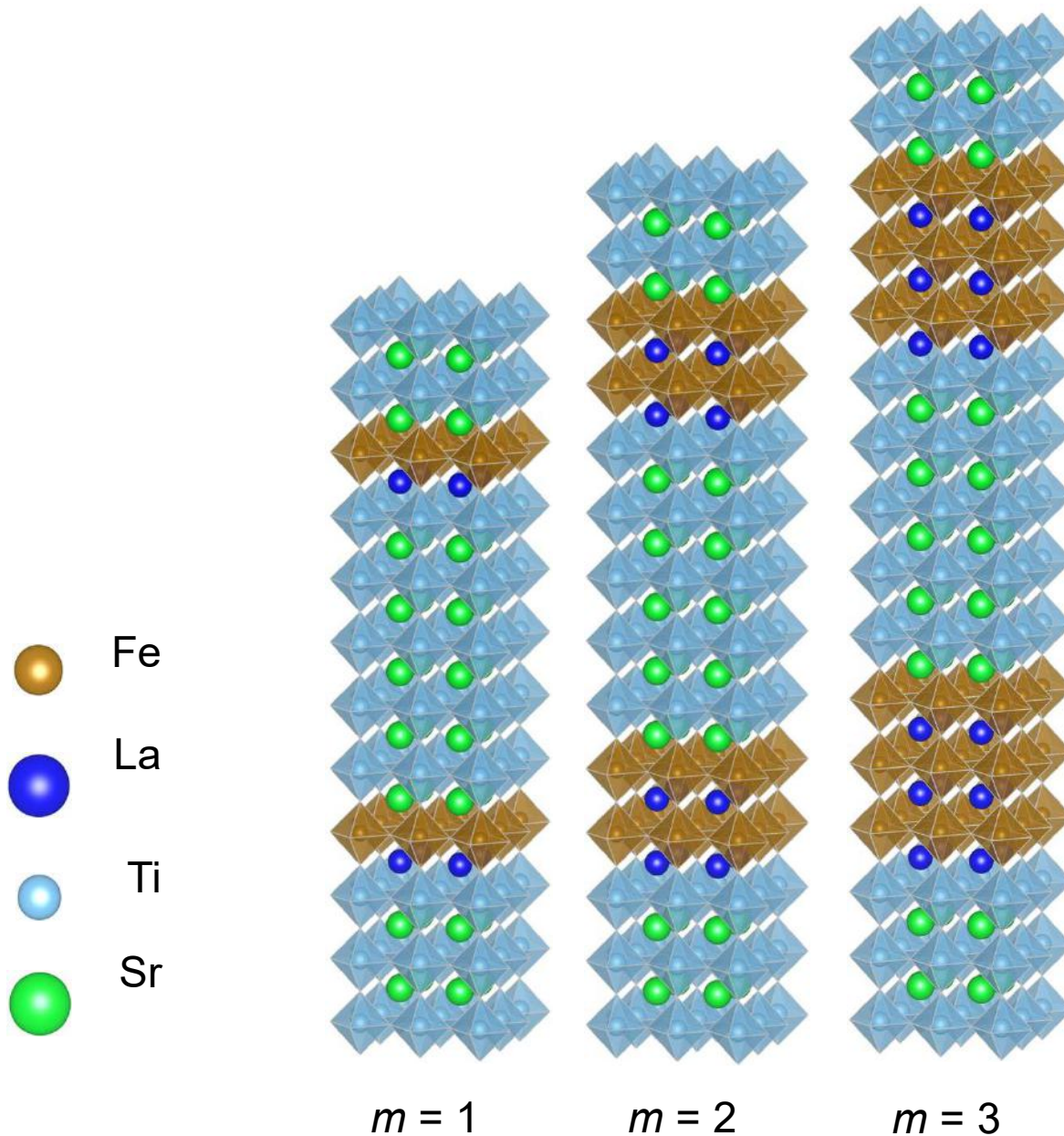
SrTiO₃ substrate

(1+1)x10 superlattice



Profile from AFM image show vicinal steps
From fit (not shown) of steps planes is the high
of the step $4\text{\AA} \pm 0.1\text{\AA}$ in comparison, lattice
constant of LaFeO_3 on SrTiO_3 is 3.91\AA

LaFeO₃/SrTiO₃ superlattices

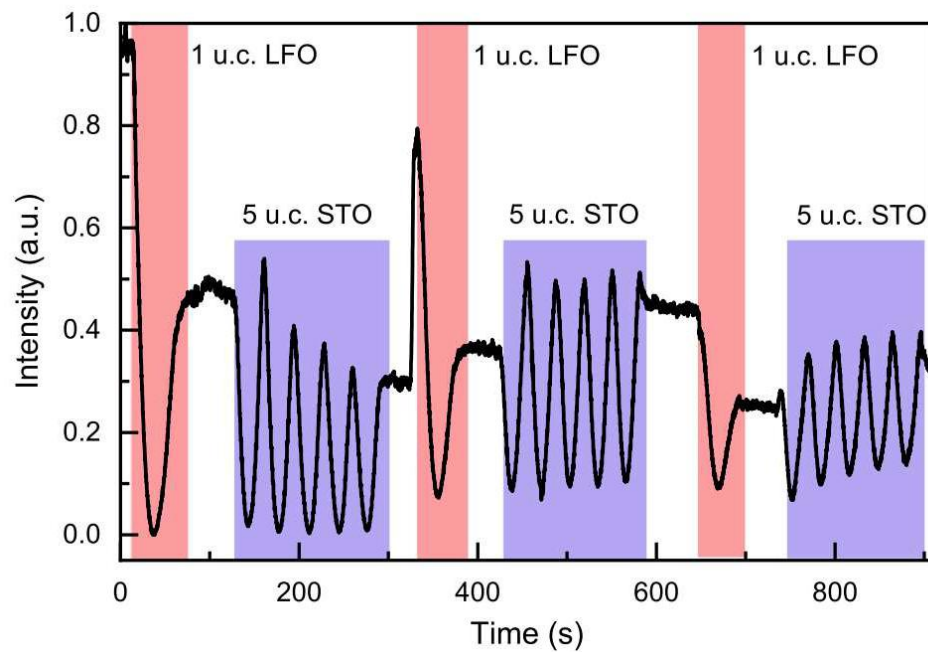


Magnetic properties of LaFeO₃ in 2D?

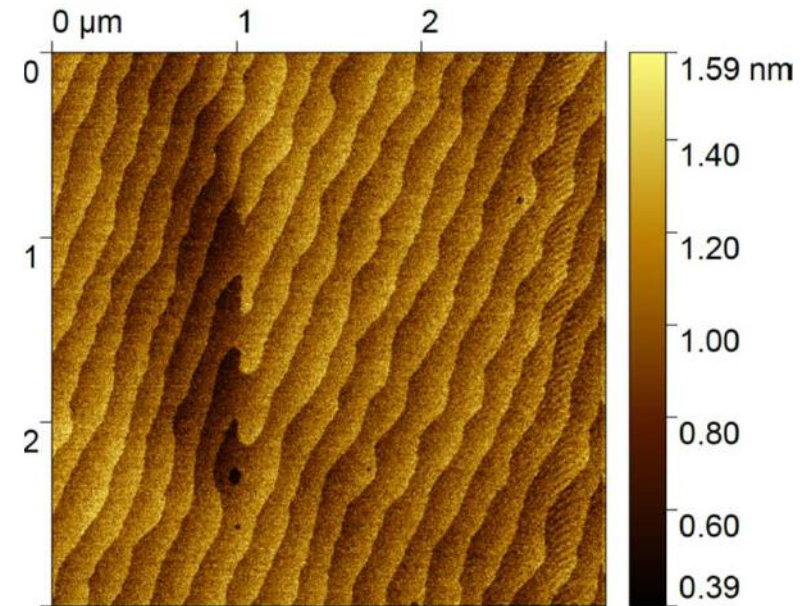
- LaFeO₃ – G type antiferromagnet with a high Néel temperature of 740 K
- SrTiO₃ spacer – nonmagnetic semiconductor

Growth and surface of $\text{LaFeO}_3/\text{SrTiO}_3$ superlattices

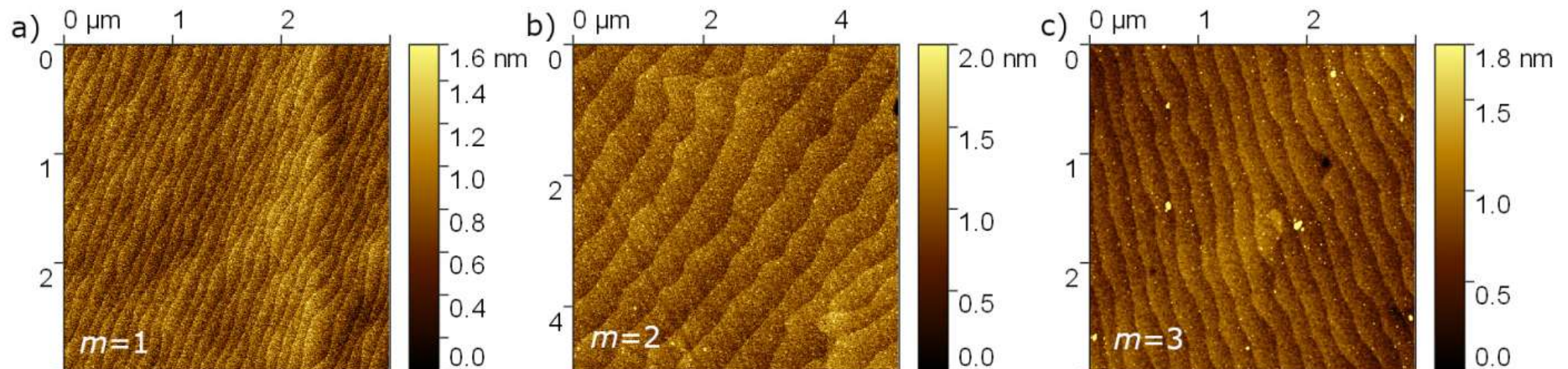
RHEED oscillations during growth



AFM images of SrTiO_3 surface

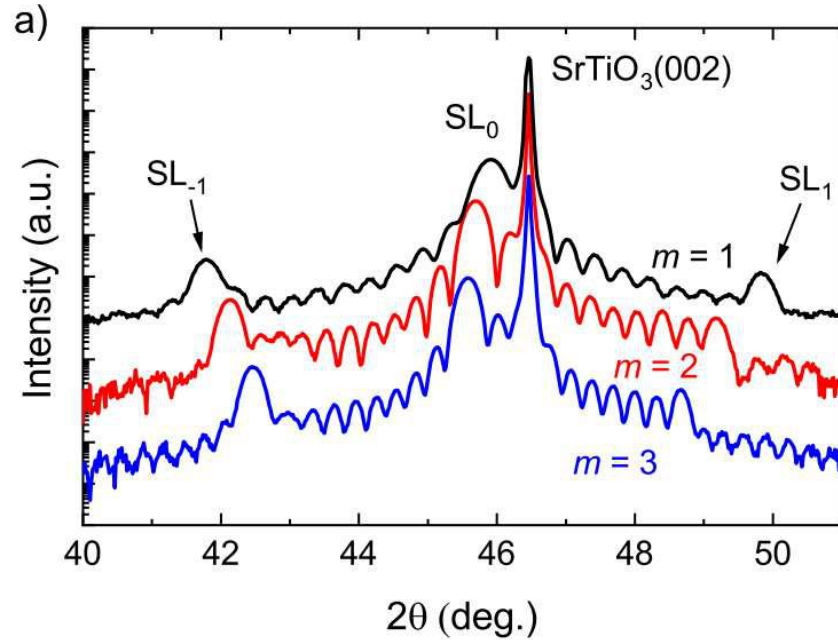


AFM images of superlattices

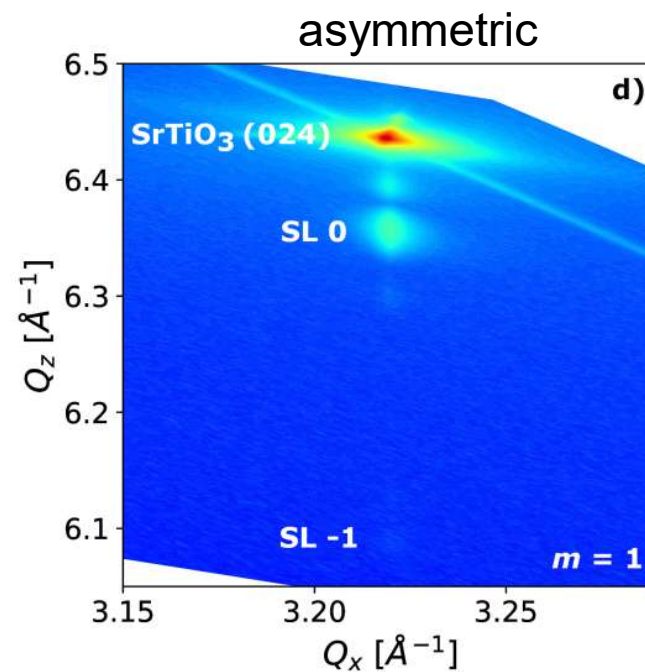
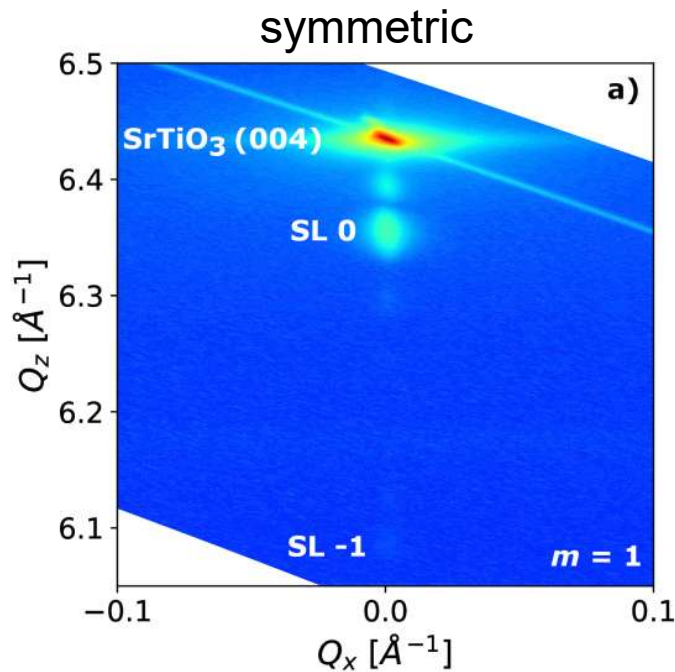
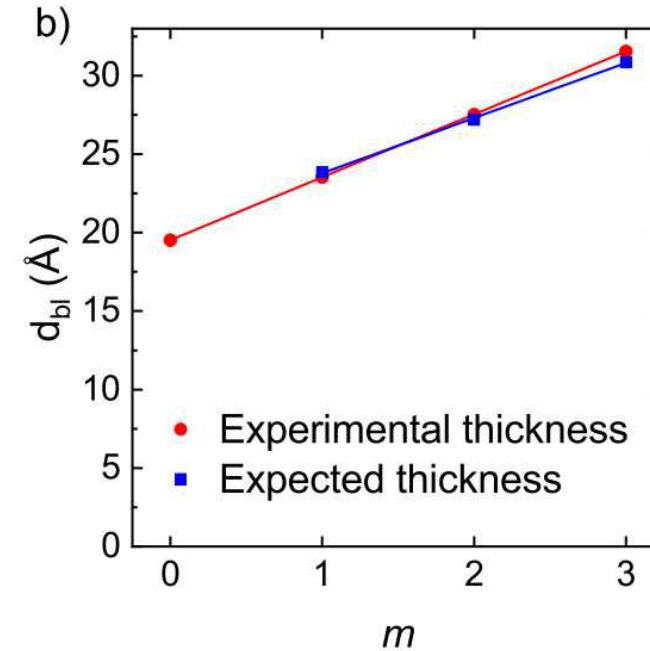


X-ray results on LaFeO₃/SrTiO₃ superlattices

Diffraction on superlattices

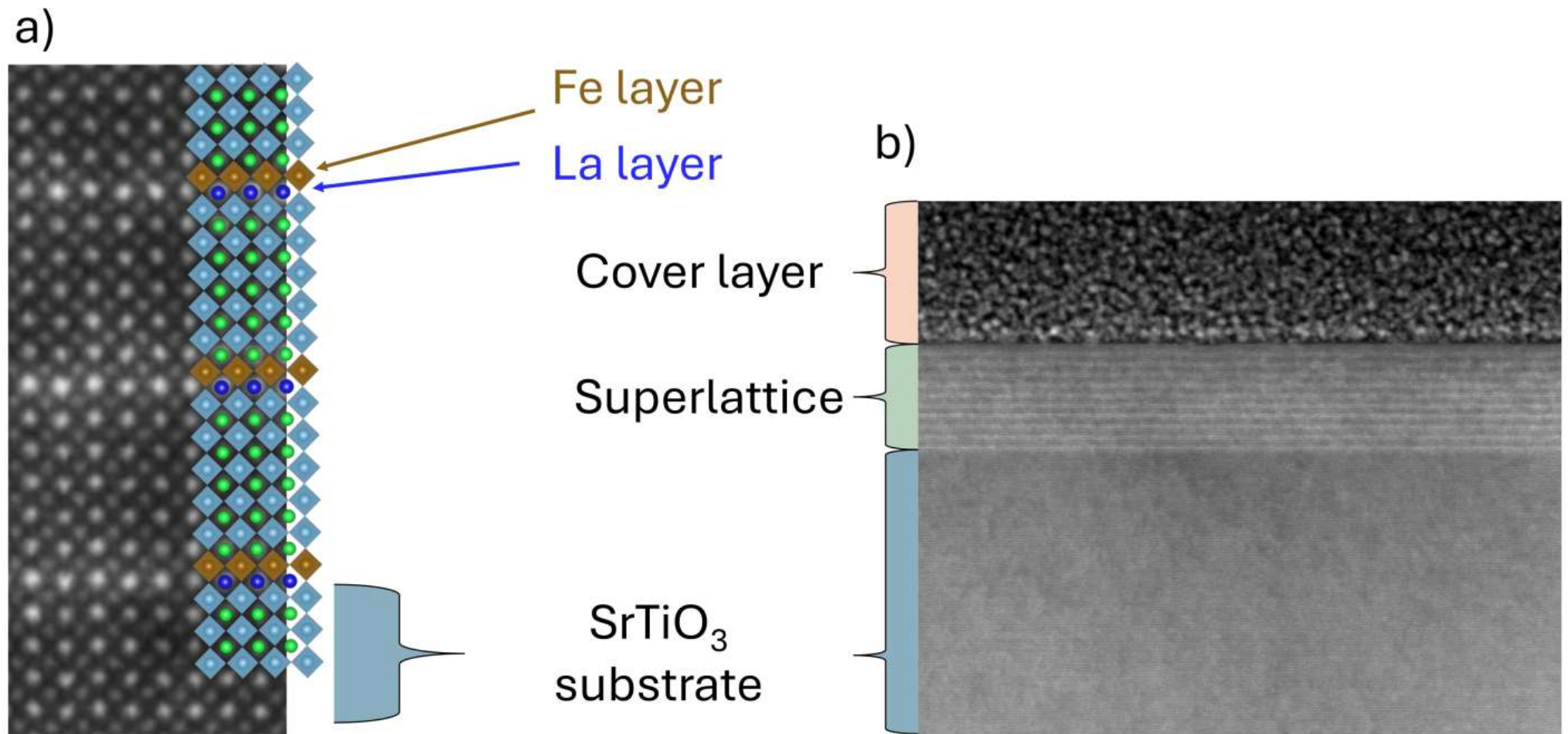


Thickness of bilayer form diffraction

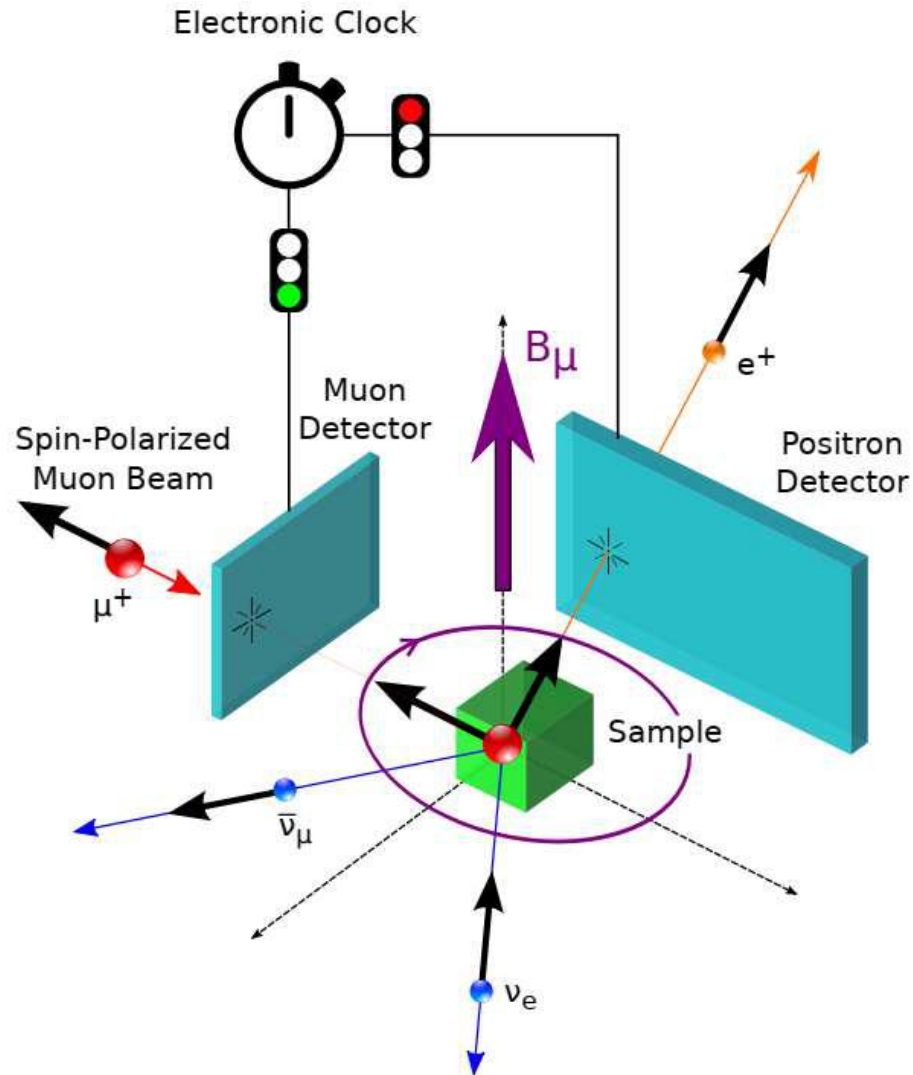


Diffraction maps demonstrate epitaxial structure

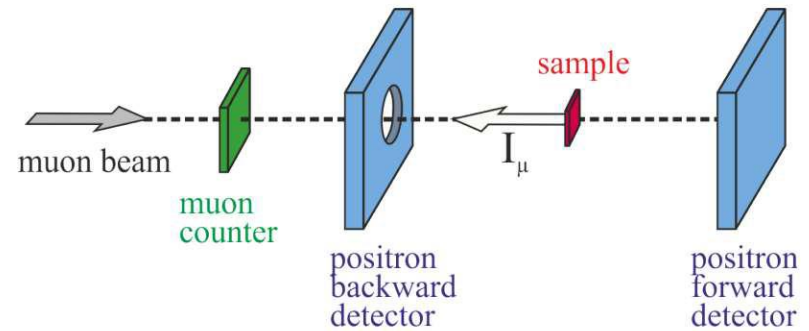
TEM of $\text{LaFeO}_3/\text{SrTiO}_3$ $m=1$ superlattice



Muon spin rotation spectroscopy (PSI, Villigen)



Drawing A. Suter, PSI



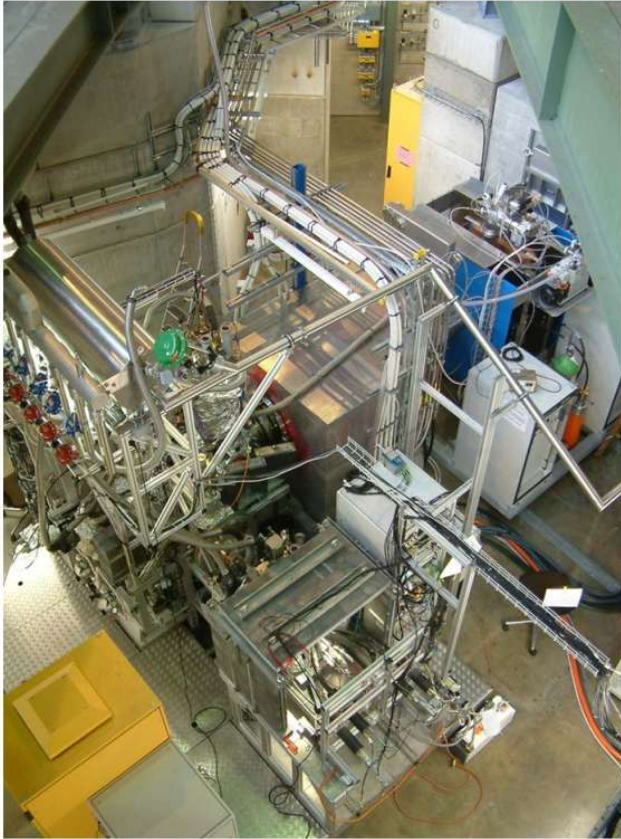
A. Amato, Physics with muons

Data displayed in terms of asymmetry between detectors (front-back, up-down)

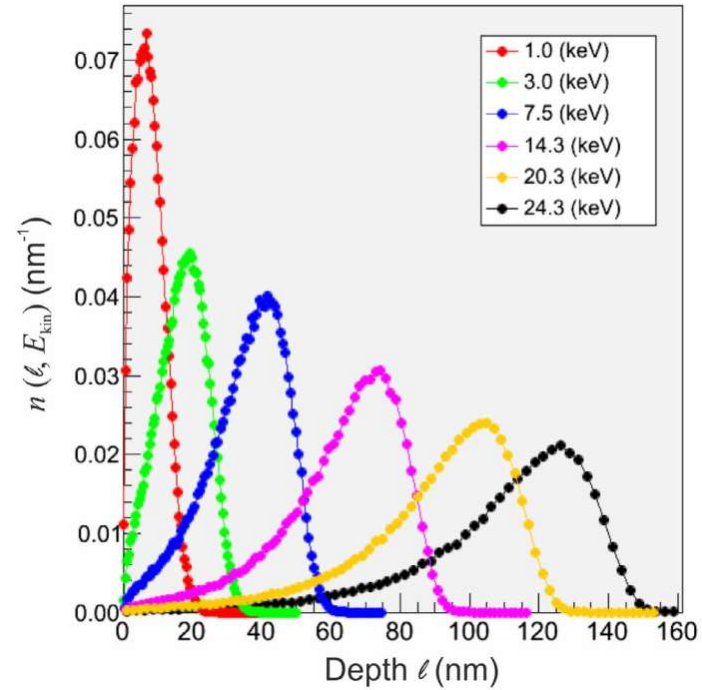
$$A(t) = A_0 P(t) = \frac{N_B(t) - N_F(t)}{N_B(t) + N_F(t)}$$

- Determination of magnetic volume fraction static magnetic order (weak transverse field measurements)
- Differentiation between static disorder and fluctuating magnetic moments (longitudinal field measurements)

Low-energy muon spin rotation (PSI, Villigen)

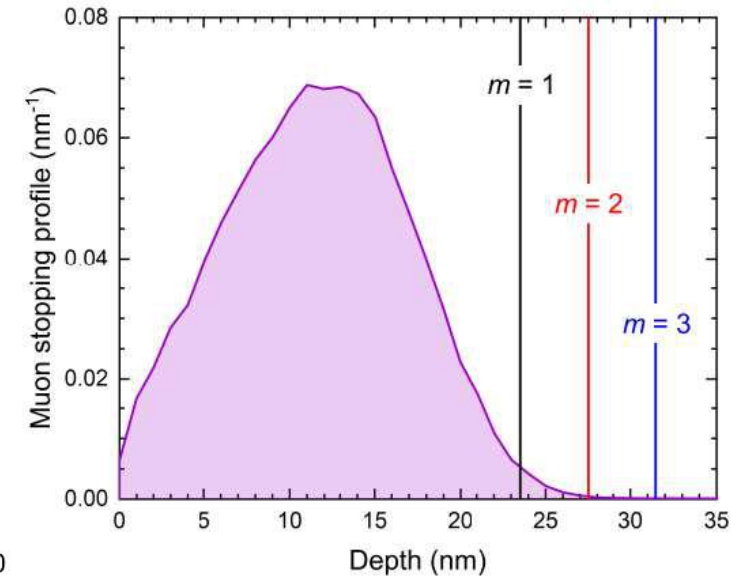


World-unique low-energy muon-spin rotation instrument



Monte Carlo simulation of stopping profiles of low energy muons in $\text{YBa}_2\text{Cu}_3\text{O}_{7-\delta}$, as a function of the implantation energy

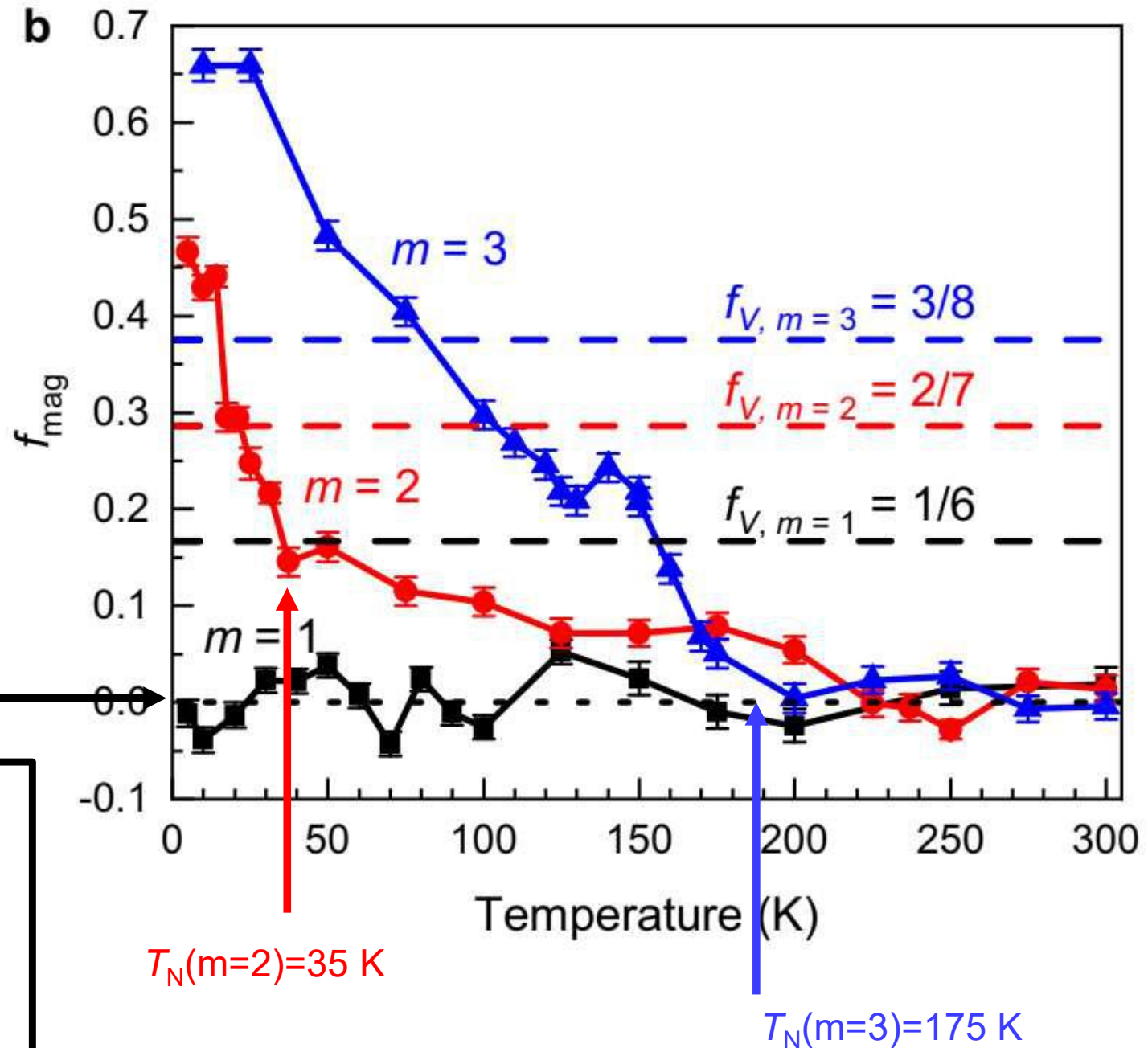
(A. Amato, Physics with muons)



2 keV beam profile just probes the volume of our superlattices

Determination of volume fraction of static magnetism from muon spin spectroscopy (weak transverse field measurements)

M. Kiaba.. and A.D., Nature Communications, 15, 5313 (2024).



Can we differentiate between static disorder and fluctuating moments?

Summary

- Pulsed laser deposition is a powerful technique that can be used for the growth various compounds
- Transition metal oxides can be grown with monolayer control using RHEED
- Essentially atomically flat surfaces can be obtained

